A Light for Science

European Synchrotron Radiation Facility

Surface and Interfaces Studied with X-ray Standing Waves, Diffraction and Spectroscopy

Jörg Zegenhagen

ESRF Grenoble, France

- (Hard X-ray) photoelectron spectroscopy (HA)XPES, XSW and SXRD at the ID32 beamline :

Complementary surface science tools and efficient use of beamtime

- X-ray diffraction and electrochemical interfaces
- XSW element specific imaging (dilute samples)
- XSW and ESCA 1/3 ML Sn phase on Ge(111)
- Structure and Fermi edge of doped $SrTiO_3$ and $SrTiO_3/LaAlO_3$ interfaces
- Concluding remarks

ESCA = electron spectroscopy for chemical analysis

XSW = X-ray standing waves

HAXPES = hard X-ray photoelectron spectroscopy

Schematic Beamline Layout

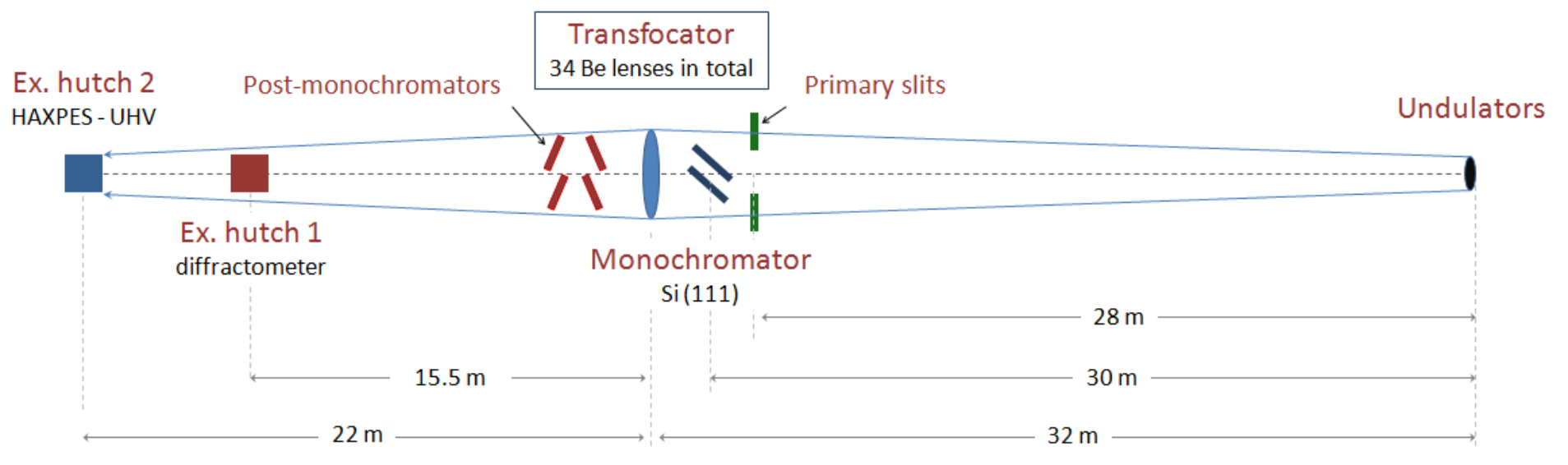

Surface X-Ray diffraction setup at ID32

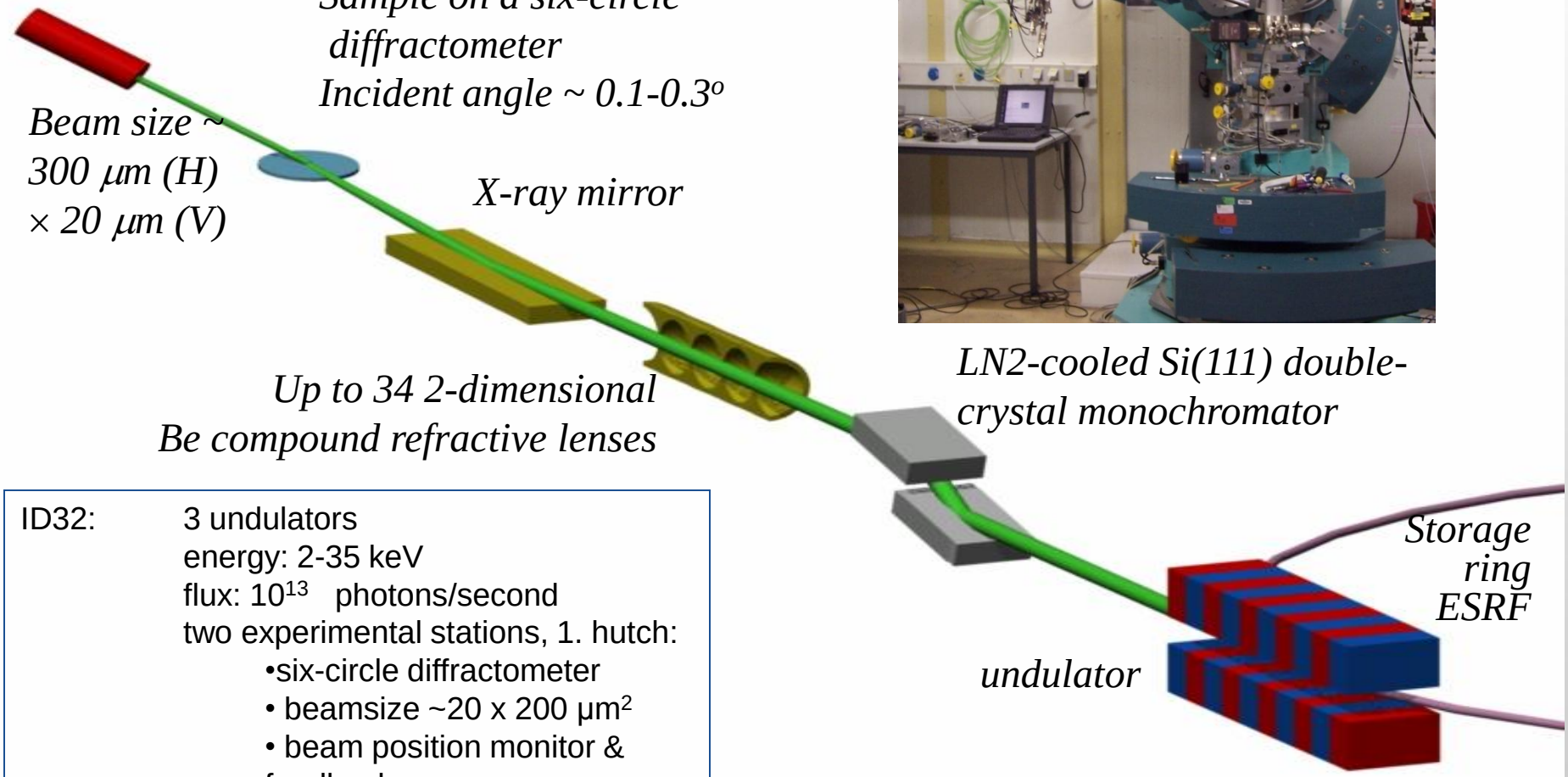

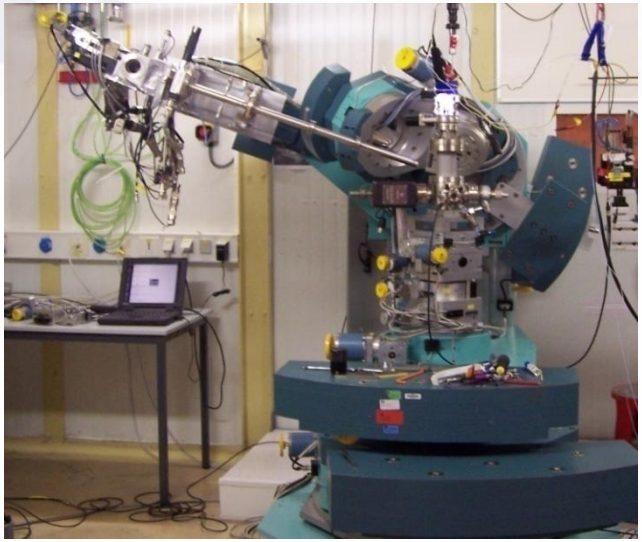

ID32: 3 undulators
energy: 2-35 keV
flux: 10^{13} photons/second
two experimental stations, 1. hutch:
- six-circle diffractometer
- beamsize ~20 x 200 μm^2
- beam position monitor & feedback

Structure of C_{60} on Ge(111)

UHV surface X-ray crystallography at ID32

C_{60} molecule

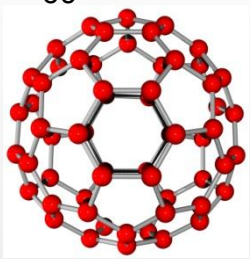

Preparation in The SCL
Deposition on Clean Ge(111) -c(2x8), annealing to about 500C

LEED image

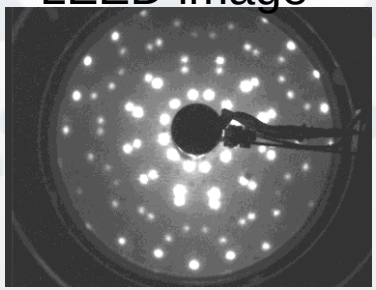

STM image

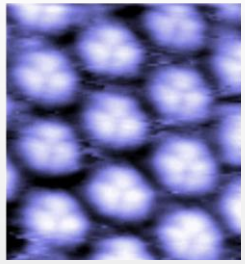

Transfer into baby chamber, GIXRD measurement in UHV on the ID32 6-circle diffractometer, about 2000 structure factors; data analysis using direct methods

Electron desity map

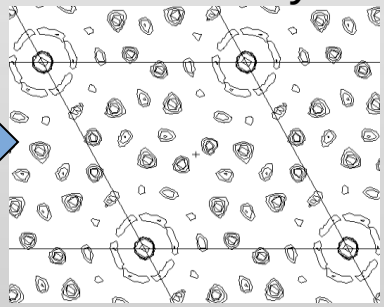

Resultant structure

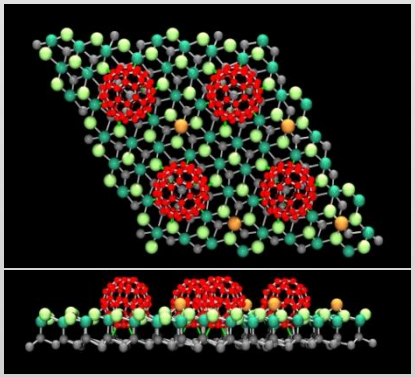

Calculated STM image

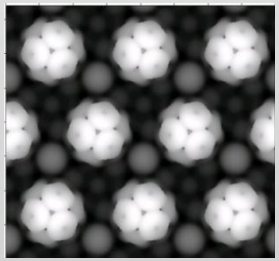

X. Torrelles, T.-L. Lee, J. Rius, O. Bikondoa, P. Ordejon, E. Machado, J. Zegenhagen, ESRF Highlights 2003, ESRF Newsletter June 2004

Electrochemistry at realistic speed

High-speed *in situ* surface X-ray diffraction studies of the electrochemical dissolution of Au(001)

F. Golks, K. Krug, Y. Gründer, J. Zegenhagen, J. Stettner, O. Magnussen:
Journal of the American Chemical Society ***133***, 3772 (2011).

Dissolution studied at around 1 V
(Beyond the range of this volammogram)

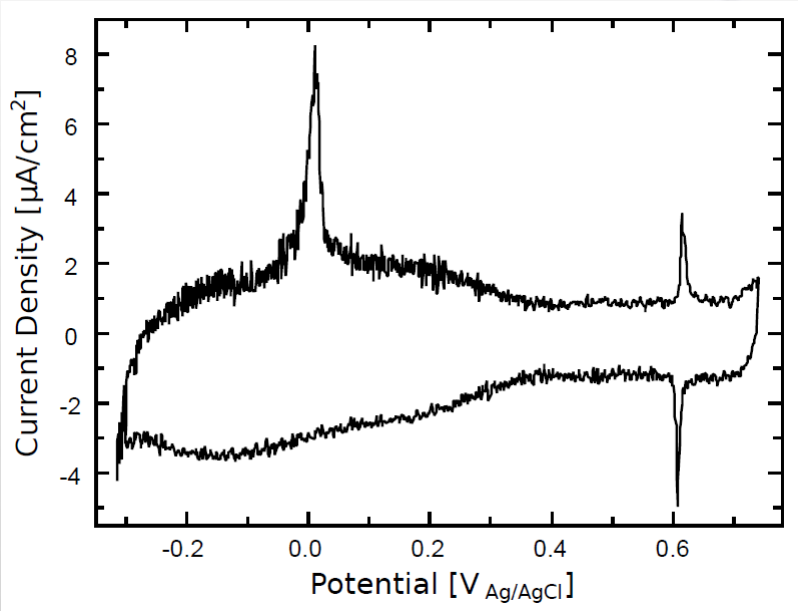

Cyclic voltammogram of Au(001) in 0.1 M HCl (dE/dt=20mV/s), showing three characteristic current peaks: With increasing potential, the transition from the hexagonal reconstructed to the unreconstructed surface is observable at 0V and the disorder to c(2×*p)R45 order phase transition* of the chloride adlayer at 0.6 V.

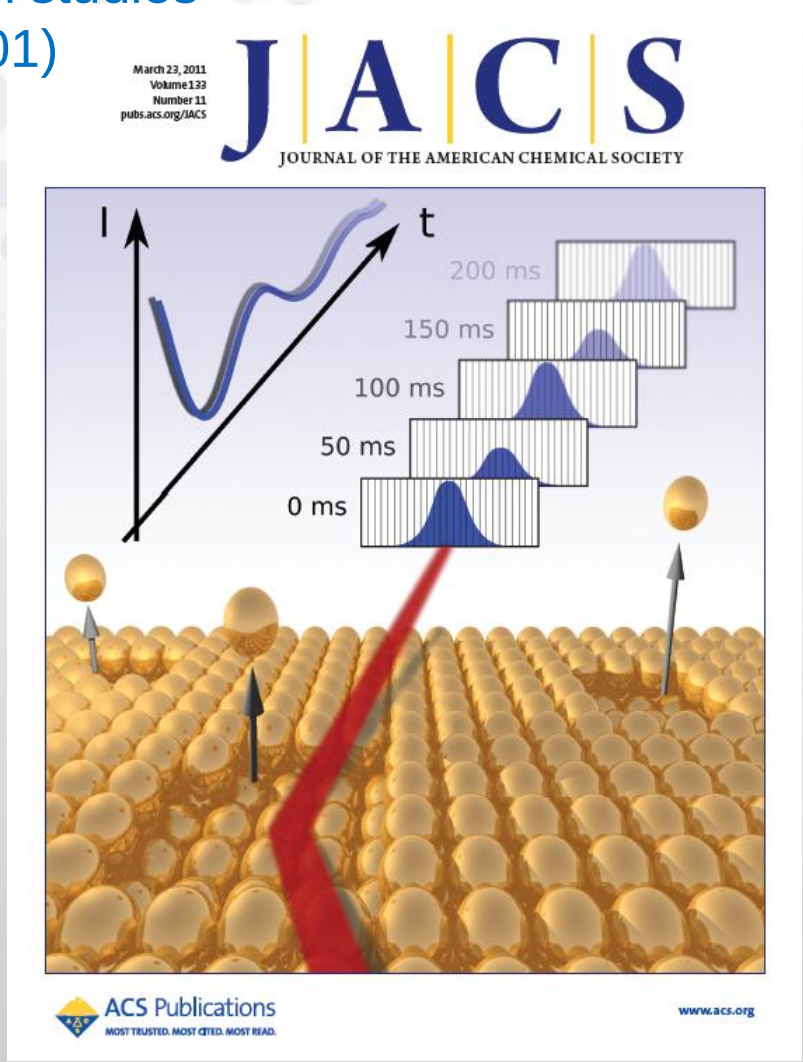

X-Ray diffraction set-up at beamline ID32 : Point detector & 1D Pixel detector

Mythen 1D detector
1280 pixel “stripes”
fast acquisition time up to 200 Hz

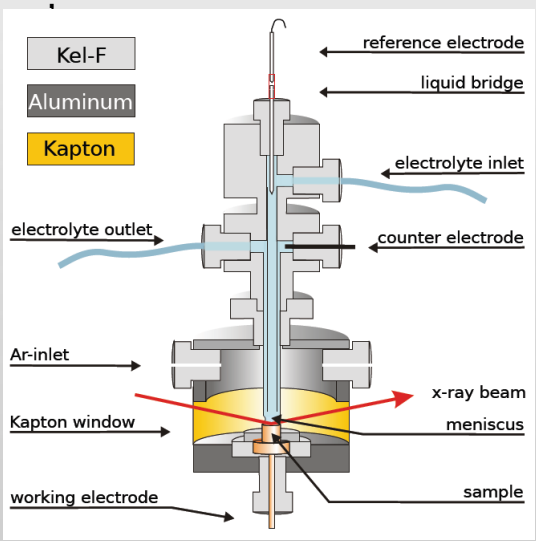

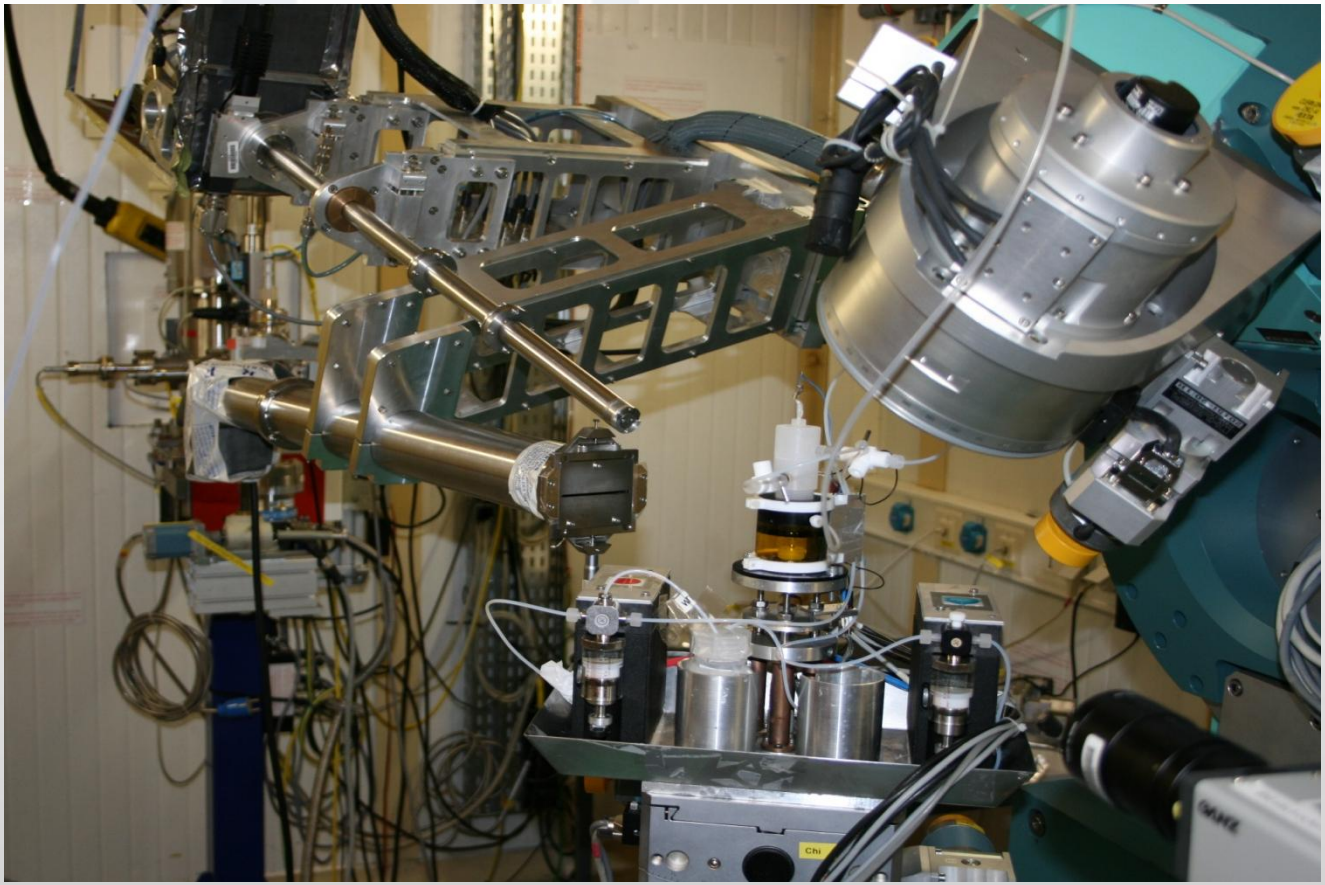

Crystal surface 4 mm Beam size 20 x 200 μm^2

Technical Documentation Mythen1K Detector System, DECTRIS Ltd.

Electrochemical dissolution of Au(001)

- time resolution of 5 ms
- layer-by-layer dissolution for entire active dissolution regime
- dissolution rates > 20 ML/s

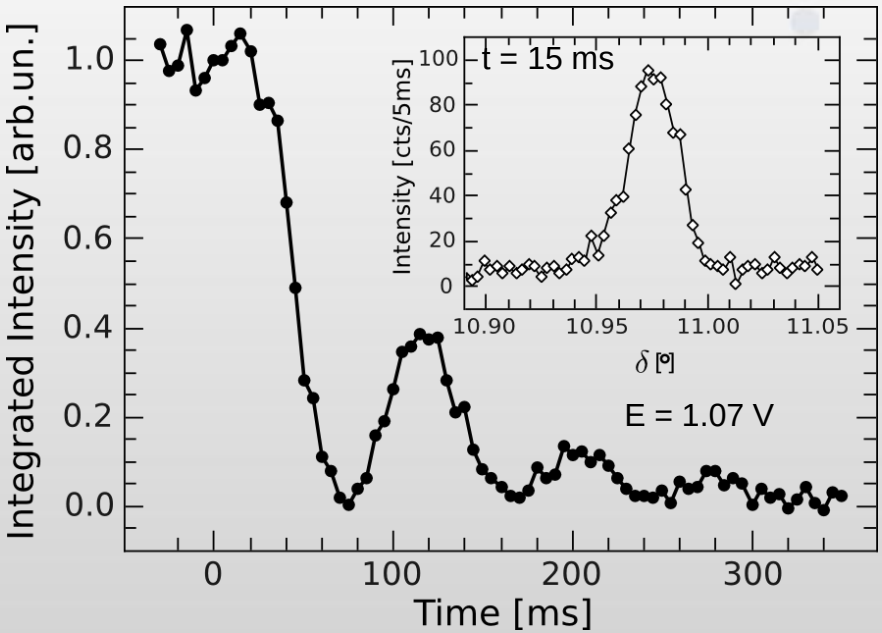

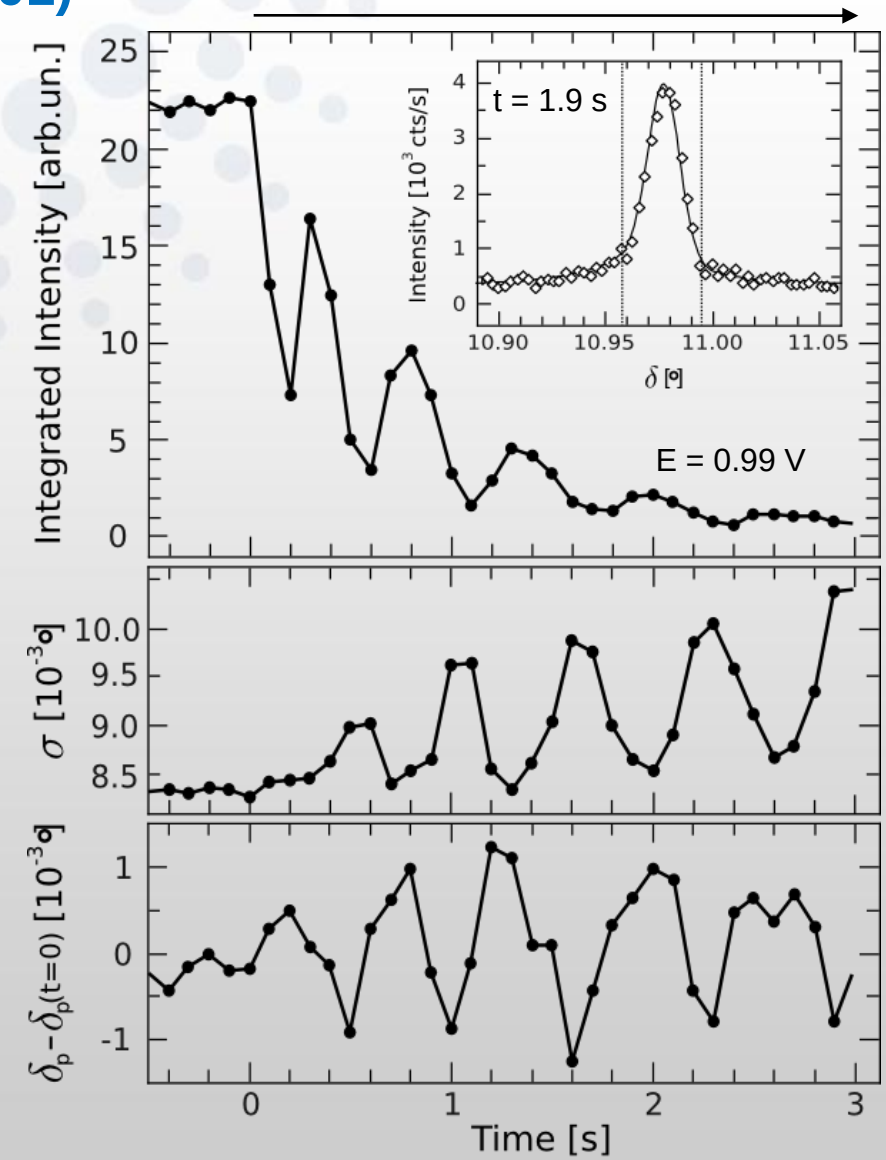

Use of fast 1D detector:
→ more information :
lateral morphology

X-ray Standing Wave Analysis

Yield: $Y(\theta) \propto 1 + R(\theta) + 2\sqrt{R(\theta)} \cdot f_H \cdot \cos[\nu(\theta) - 2\pi P_H]$

e.g. Fluorescence

Reflectivity — Coherent fraction — Phase difference — Coherent position

Element-specific "structure factor": $\mathbf{G_H} = \int_{V_{uc}} \rho(\mathbf{r}) \cdot e^{2\pi i \mathbf{H}\cdot\mathbf{r}} d\mathbf{r} = f_H \cdot e^{2\pi i P_H}$

Normalized **atomic** distribution

X-ray Standing Wave Analysis of Bismuth Implanted in Si(110)
N. Hertel, G. Materlik and J. Zegenhagen
Z. Phys. B Condensed Matter 58, 199 – 204(1985).

XSW

- *measures directly phases of "structure factors"* ↔ *phase problem in diffraction*
- *is element and chemical-state specific and sensitive to low-Z elements*
- *does not require long-range order*
- *offers high spatial resolution*
- *requires good-quality crystals* → *backscattering geometry*
- *provides only folded structural information (no info on length scales* $> a_{substrate}$*)*

XSW-imaging* dopant atoms : Mn in GaAs

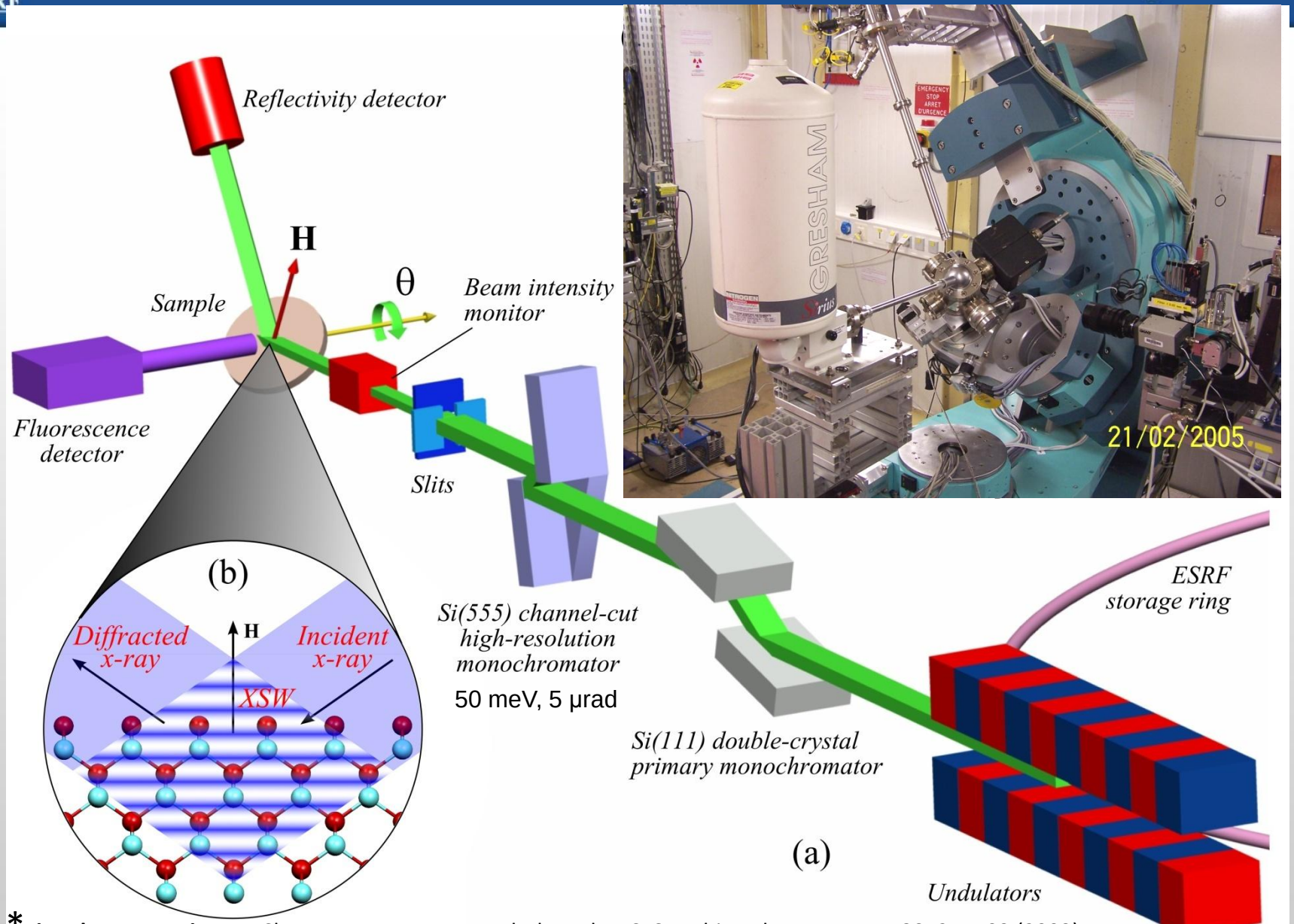

*First demonstration : L. Cheng, P. Fenter, M. J. Bedzyk, and N. C. Sturchio, Phys. Rev. Lett. **90,** 255503 (2003).

Postmono modes

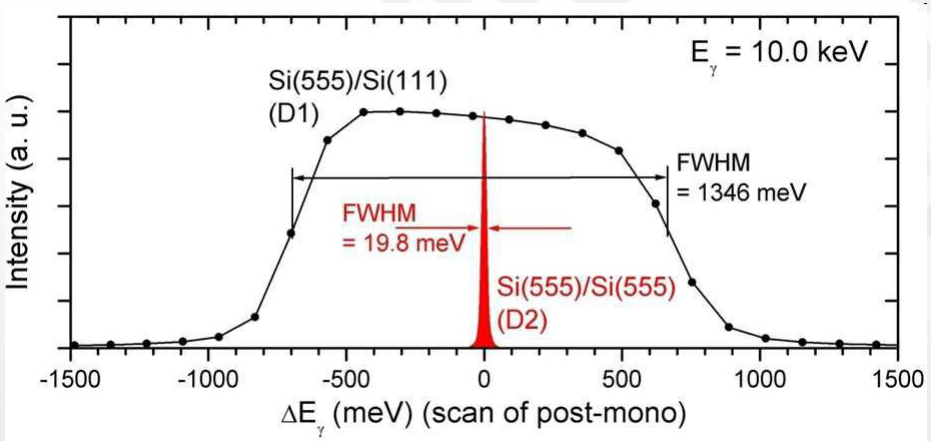

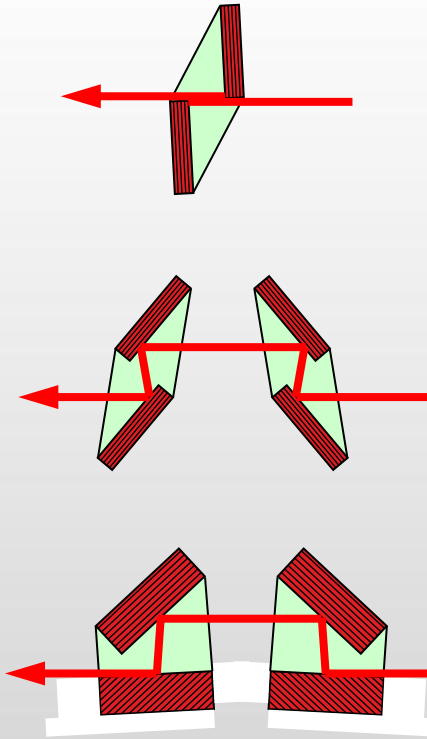

High resolution secondary monochromators in UHV ; view inside

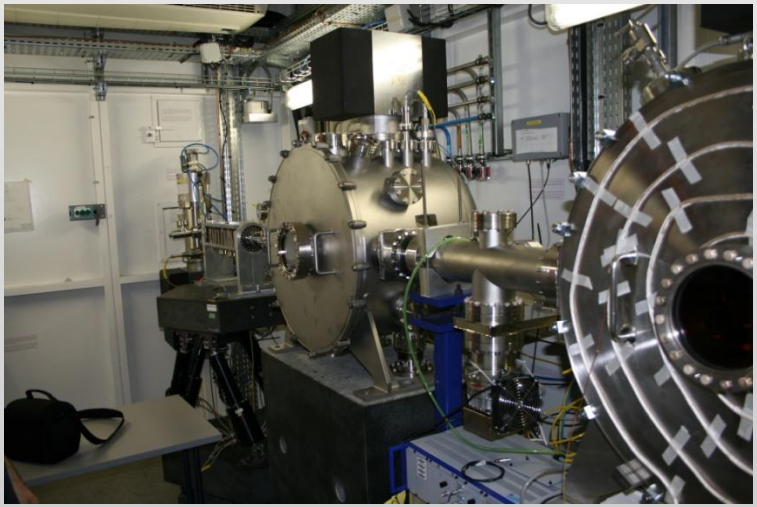

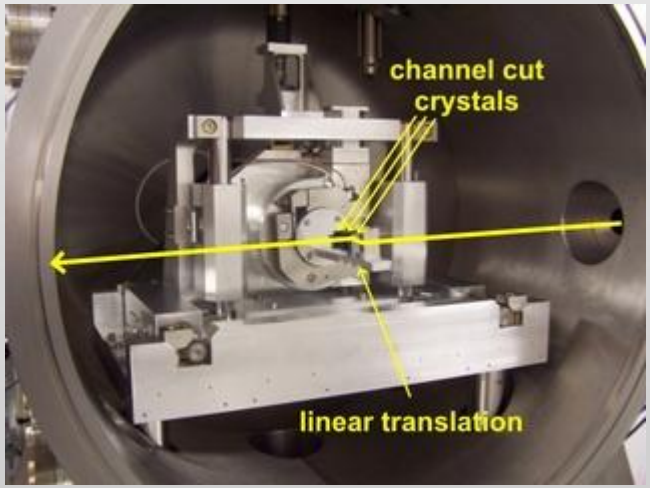

Up to five sets of channel cut crystals can be selected

XSW measurement of Mn in GaAs

(4% Mn in 4nm film on GaAs)

XSW data

16 – 22 reflections measured for each sample

Reflectivity curves

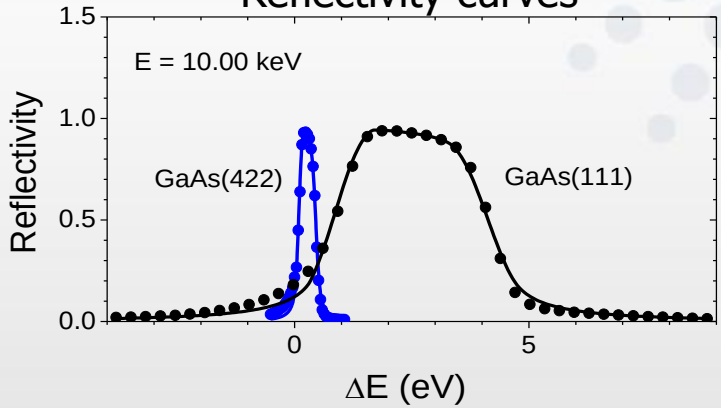

Fluorescence spectrum

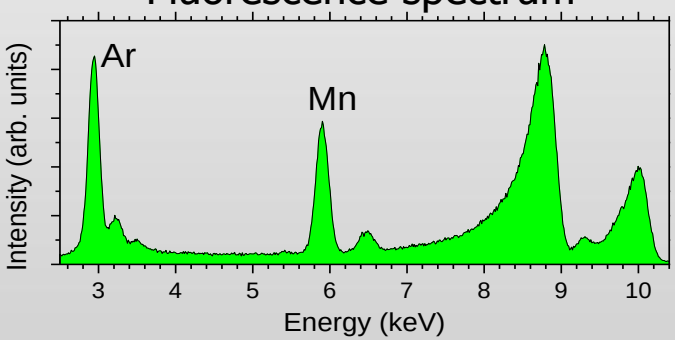

XSW modulated Mn fluorescence yield curves

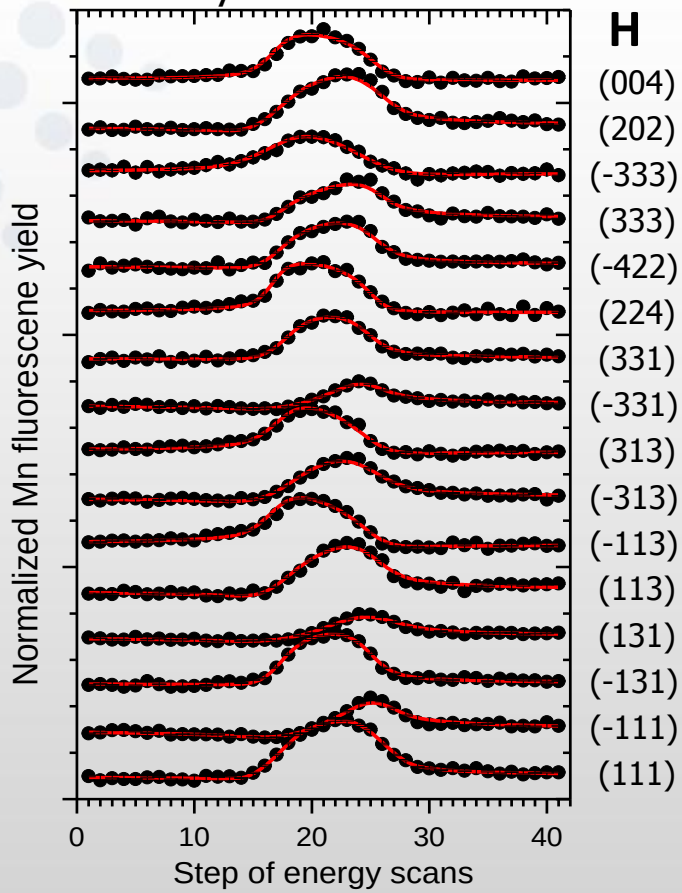

Yield: $$Y(\theta) \propto 1 + R(\theta) + 2\sqrt{R(\theta)} \cdot f_H \cdot \cos[\nu(\theta) - 2\pi P_H]$$

Reflectivity — Coherent fraction — Phase difference — Coherent position

XSW Fourier formalism:
N. Hertel, G. Materlik and J. Zegenhagen
Z. Phys. B Condensed Matter 58, 199 (1985).

XSW images of Mn position in *unit cell of GaAs*

Direct Fourier transform : $$\rho(\mathbf{r}) = 1 + 2\sum_{\mathbf{H}} f_{\mathbf{H}} \cdot \cos[2\pi i(P_{\mathbf{H}} - \mathbf{H}\cdot\mathbf{r})]$$

(a) – (c) 3-dimensional images of atomic distributions of Mn by direct Fourier transform of the element specific structure factors (amplitude AND phase) from ~20 XSW scans.

(d) - (f) Images of reconstructed from the measured Fourier components after the subtraction of the contribution of the Mn on the Ga site.
Mn on As interstitial site AND on Ga inerstitial site

(g) Ball-and-stick model of GaAs.
(h) FCC sublattices of GaAs that correspond to the Ga and As interstitial sites. The blue boxes denote the cubic unit cell of the GaAs substrate.

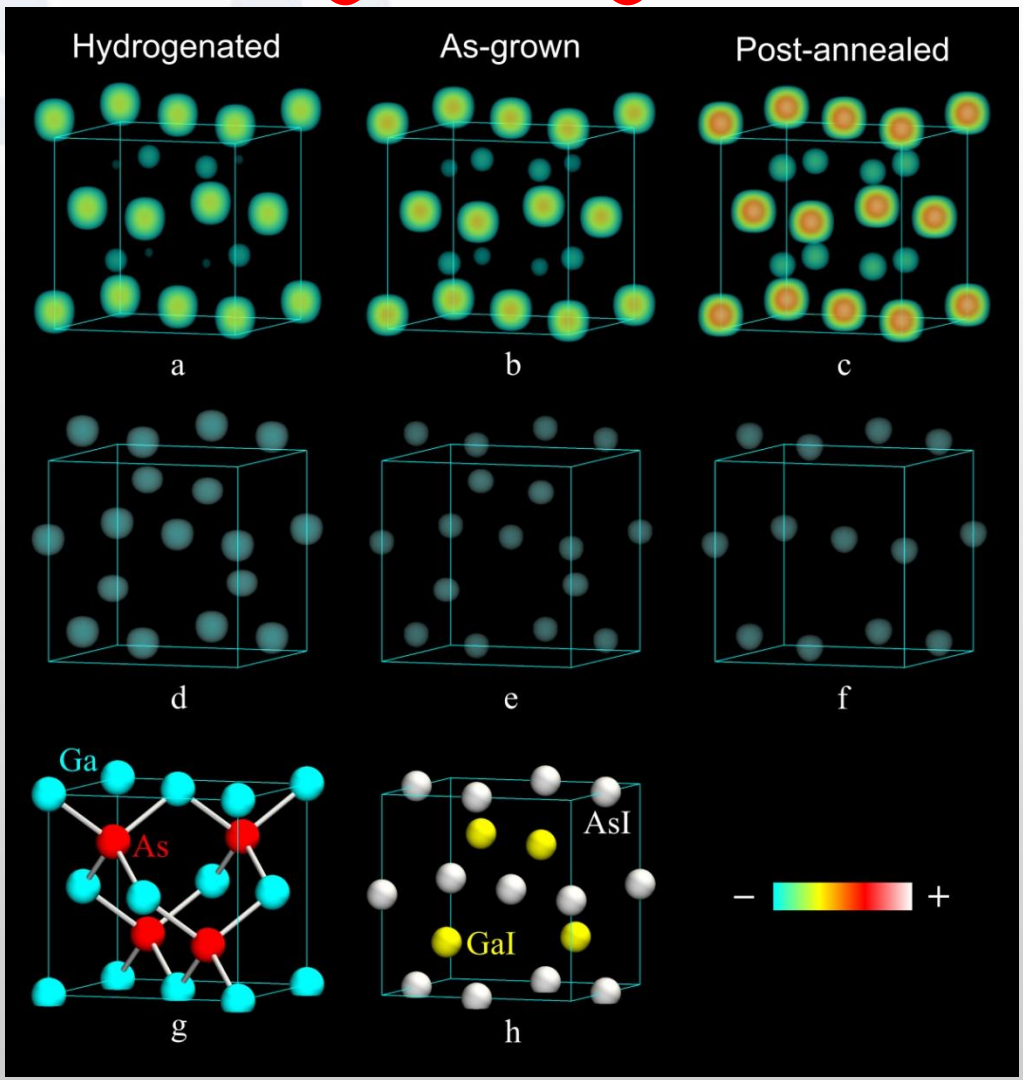

T.-L. Lee, C. Bihler, W. Schoch, W. Limmer, J. Daeubler, S. Thiess, J. Zegenhagen, Phys.Rev. B. 81, 235202 (2010).

XSW measurement of Mn in GaAs : Result of refinement
(4% Mn in 20 nm film on GaAs)

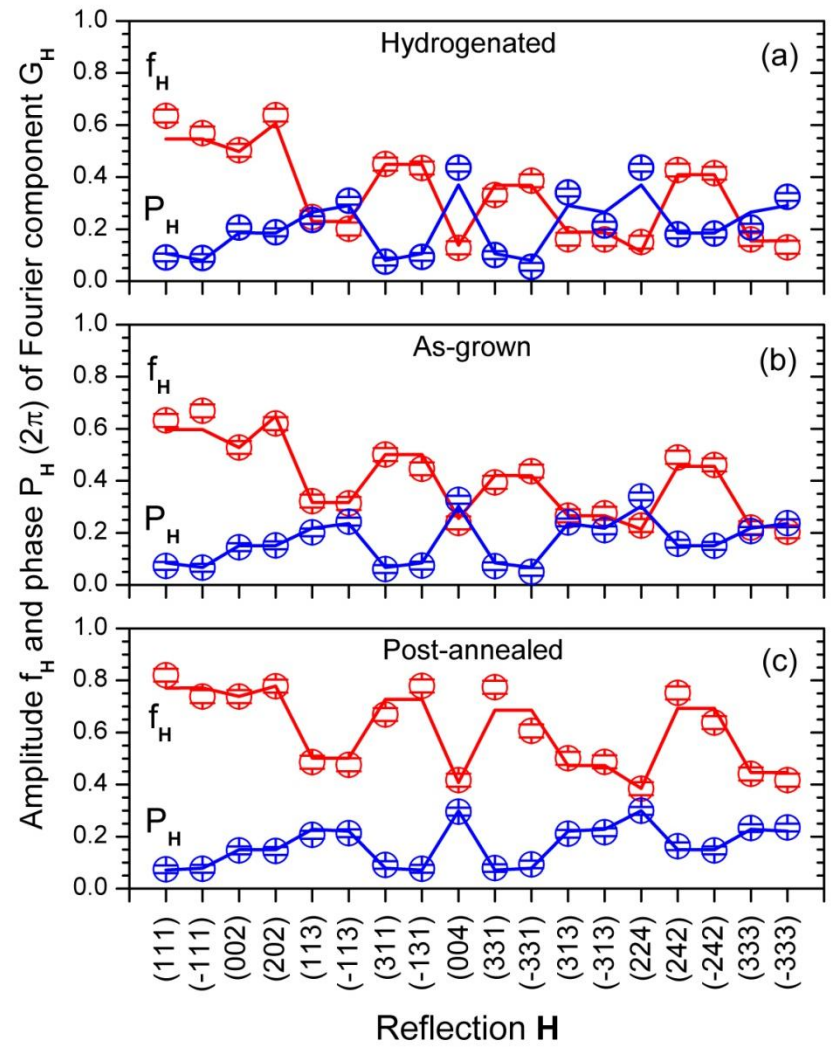

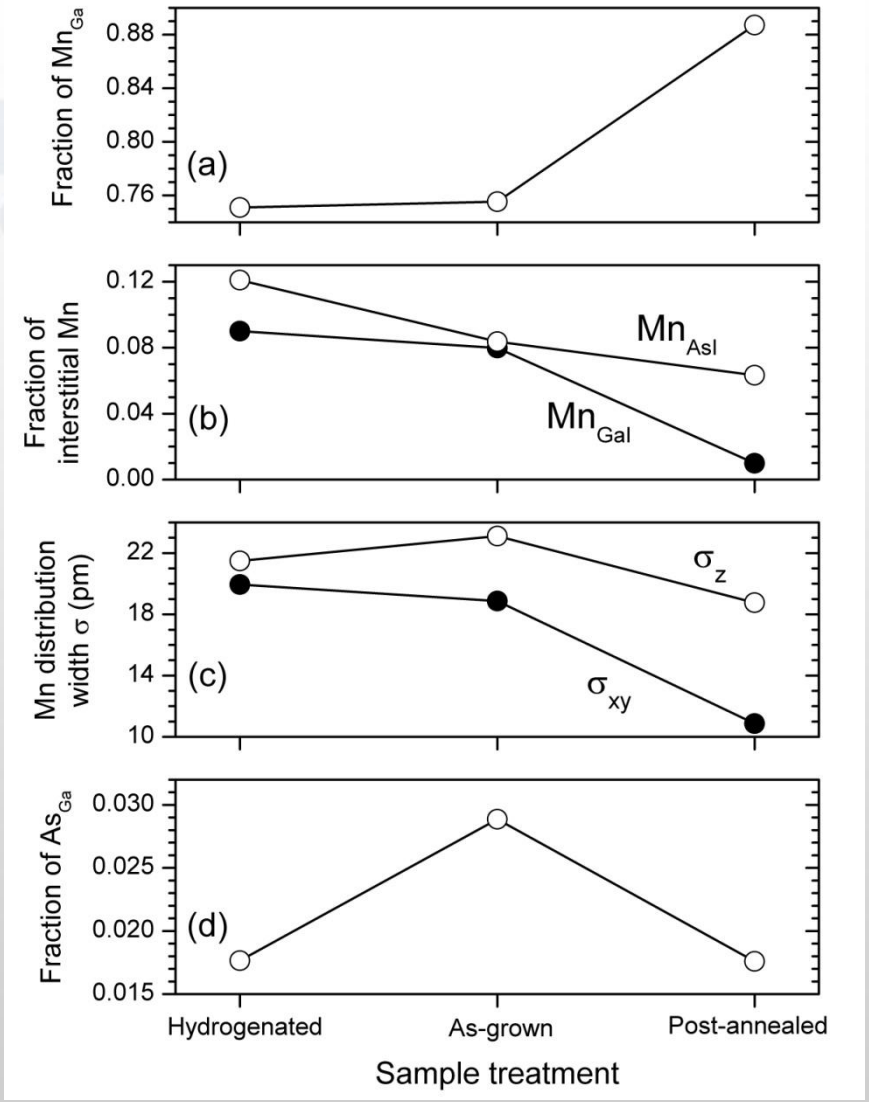

Visualizing Dopant Atoms in Dilute Magnetic Semiconductors
T.-L. Lee, C. Bihler, W. Schoch, W. Limmer, J. Daeubler, S. Thiess, J. Zegenhagen
Phys.Rev. B. 81, 235202 (2010).

Schematic set-up for XSW/HAXPES experiments in EH2

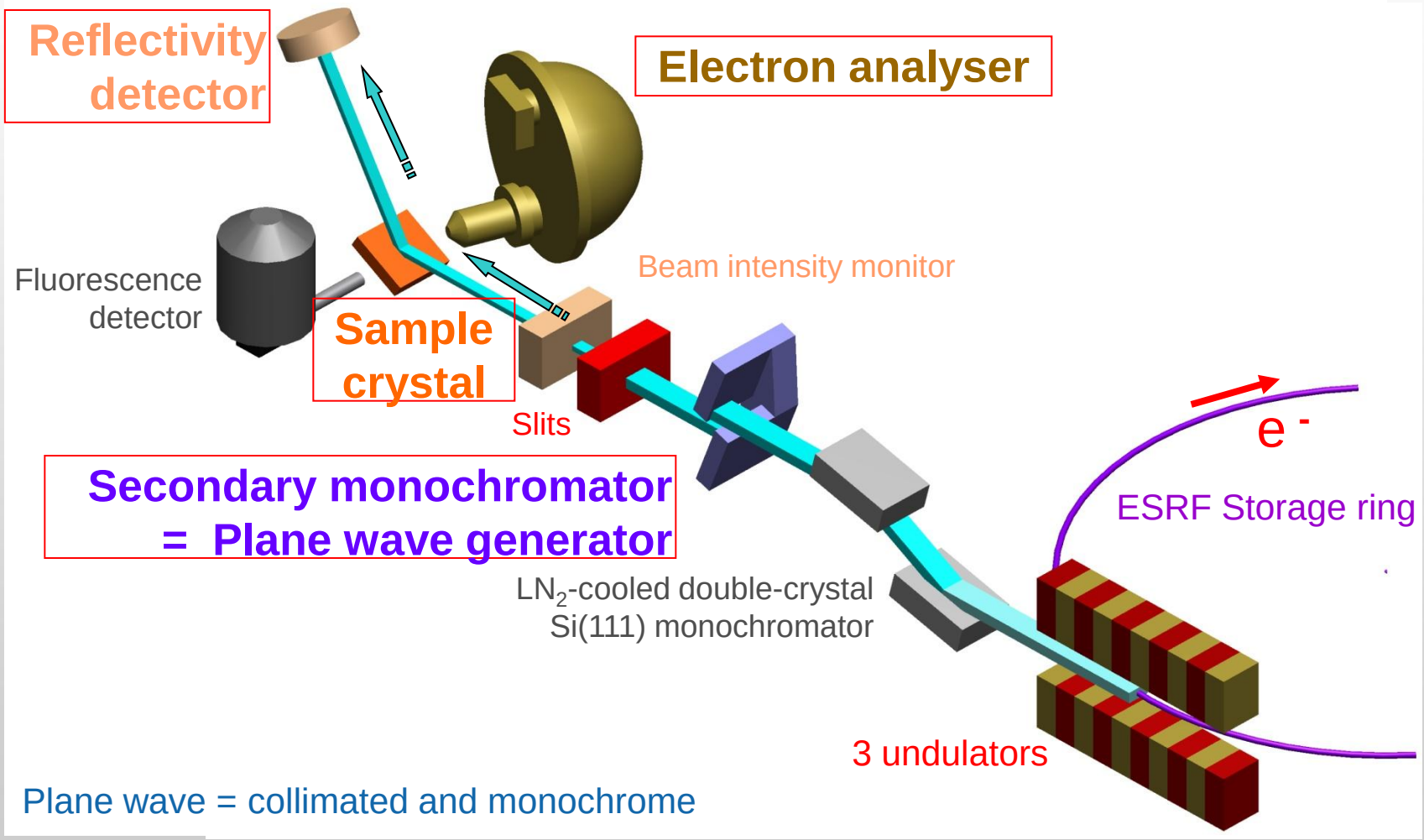

Plane wave = collimated and monochrome

J Z, B. Detlefs, T.-L. Lee, S.Thiess, H. Isern, L.Petit, L. André, J. Roy, Y. Mi, I. Joumard, J. El. Spectr. and Rel. Phenom. **178-179,** 258 (2010).

XSW/HAXPES set-up at the ID32 beamline

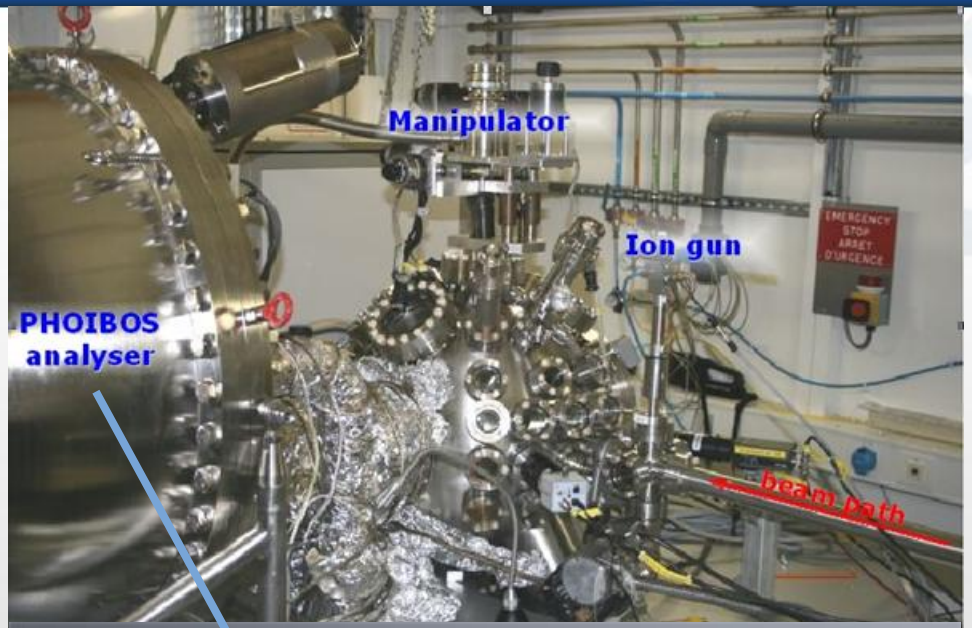

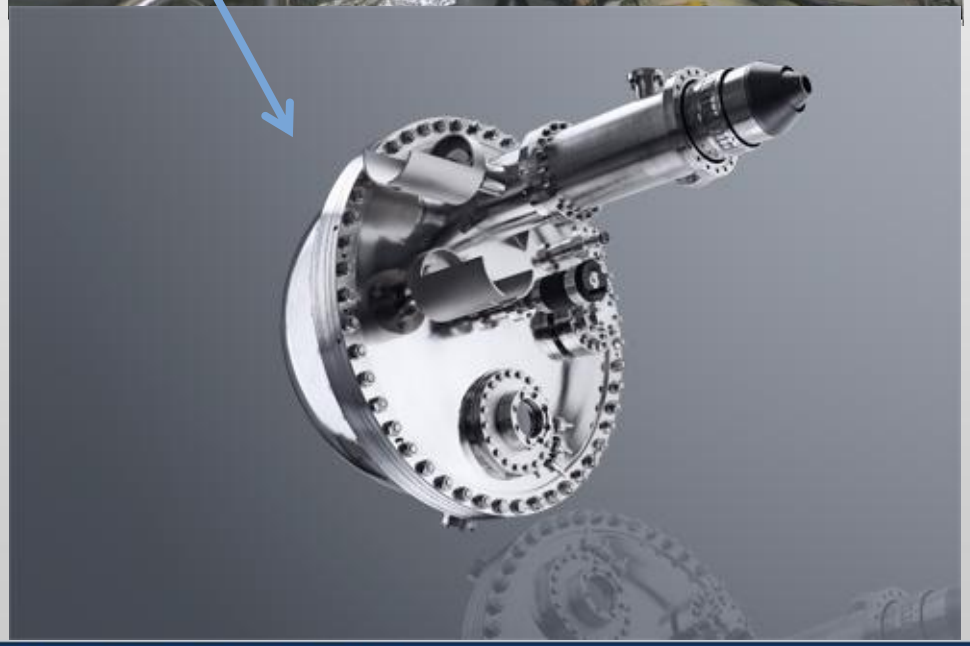

3-axes "Kappa" manipulator with x, y, z stage and detector arm during installation

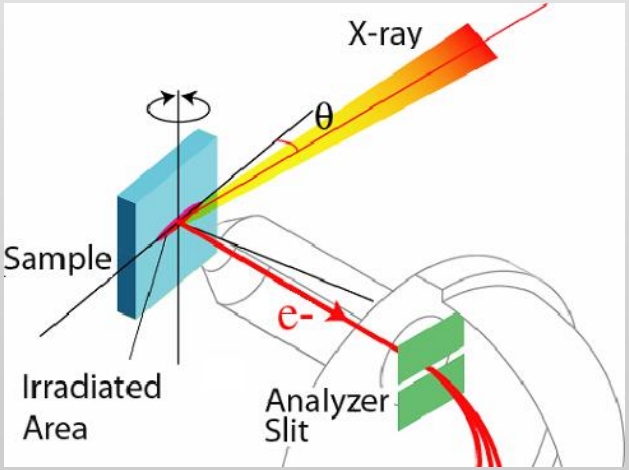

Example XSW analysis: Graphene on the Ir(111) surface

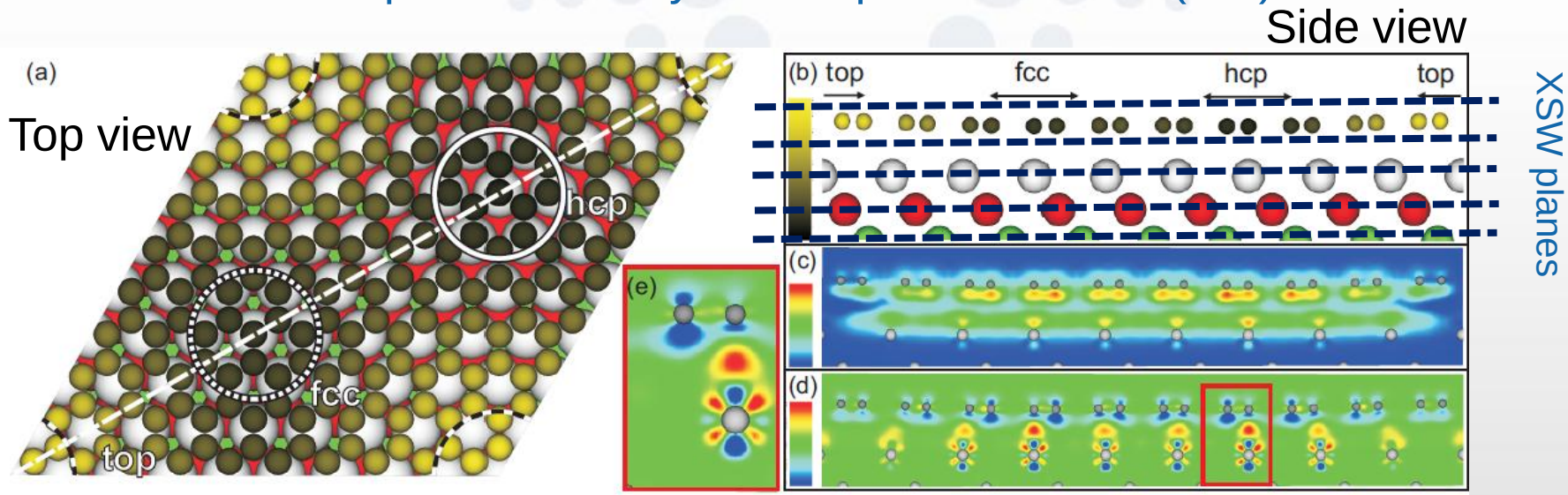

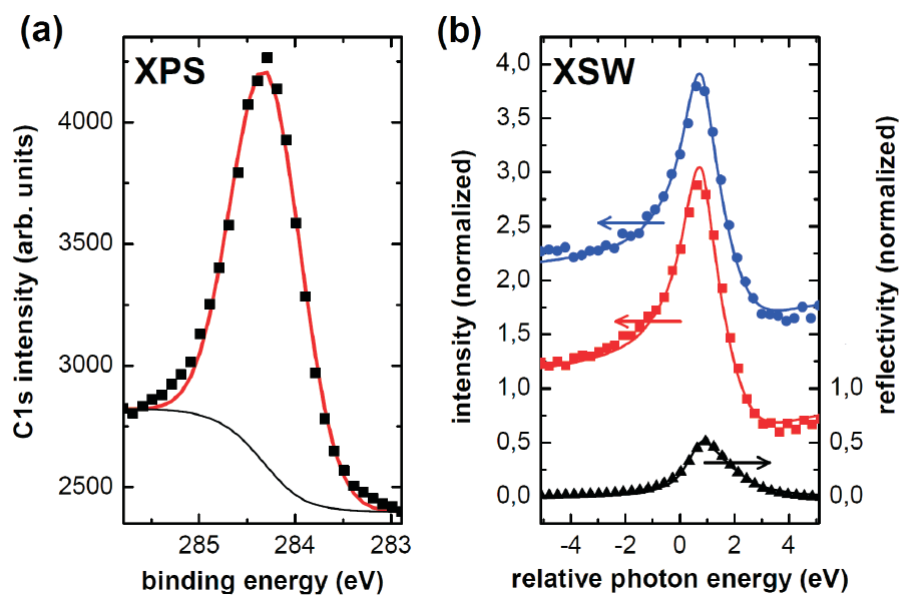

XSW result

$P^{111} = 0.53 \pm 0.01$ and

$F^{111} = 0.87 \pm 0.04$

→mean height above the surface :

$\langle h \rangle = (3.38 \pm 0.04)$ Å

Theory :

mean height $\langle h \rangle = 3.41$ Å

Busse, C.; Lazic, P.; Djemour, R.; Coraux, J.; Gerber, T.; Atodiresei, N.; Caciuc, V.; Brako, R.; N'Diaye, A. T.; Blügel, S.; Zegenhagen, J.; Michely, T. Phys. Rev. Lett. **107,** 036101 (2011,)

The Growth of the First Monolayer $YBa_2Cu_3O_{7-\delta}$ on $SrTiO_3(001)$

STM

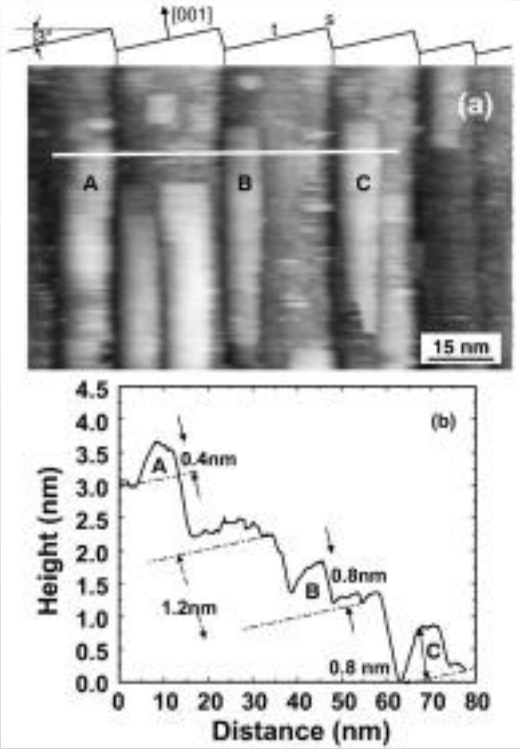

*T. Haage, J. Zegenhagen, H. –U Habermeier, M. Cardona, PRL **80**, 4225 (1998)*

$SrTiO_3$
perovskite

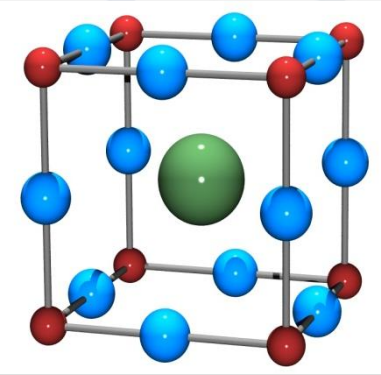

Sr
O
Ti

a = 0.391 nm

$YBa_2Cu_3O_{7-\delta}$
Superconductor, T_c = 90 K

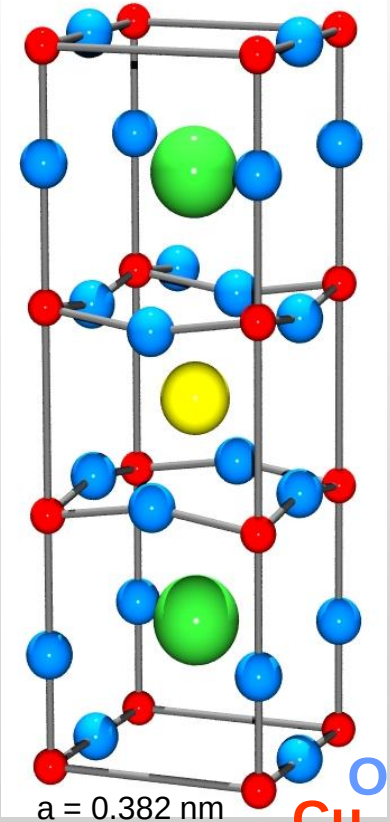

Ba
Y
Ba
O
Cu

c =1.168 nm

a = 0.382 nm
b = 0.389 nm

Experimental

- sample: 0.5 ±0.1 ML $YBa_2Cu_3O_{7-\delta}$ deposited on $SrTiO_3$(001)

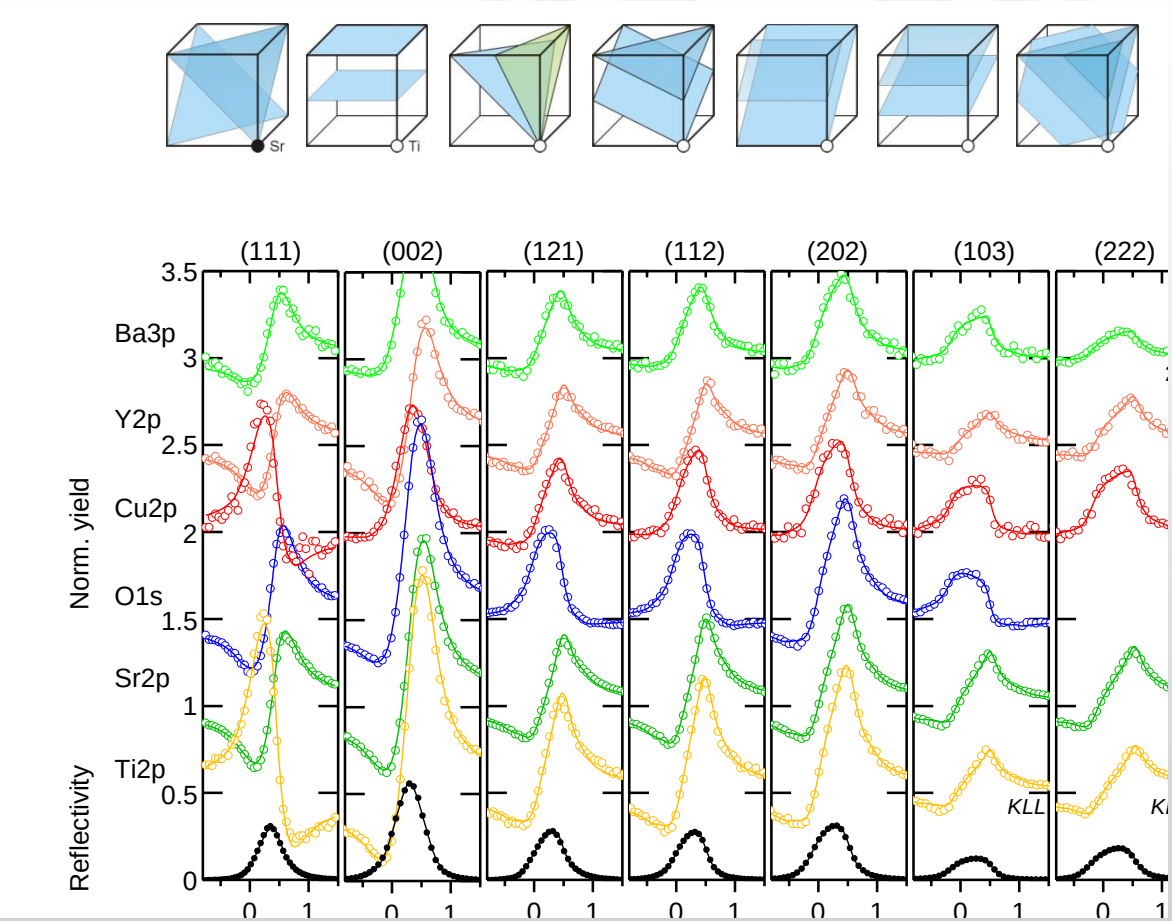

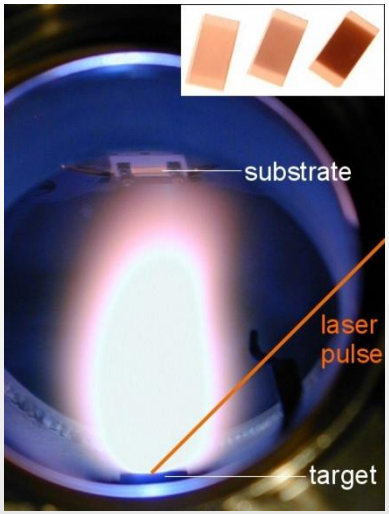

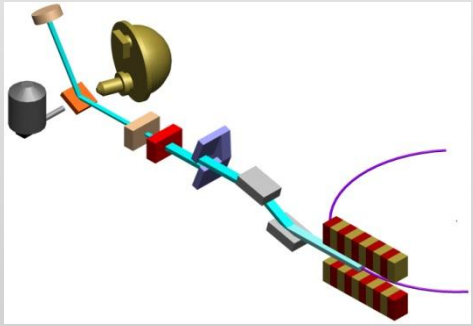

→ Reconstruction of image in real space

$$\rho(\mathbf{r}) = 1 + 2\sum_{\mathbf{H}} f_{\mathbf{H}} \cdot \cos\left[2\pi\left(P_{\mathbf{H}} - \mathbf{H}\cdot\mathbf{r}\right)\right]$$

3D reconstructed images

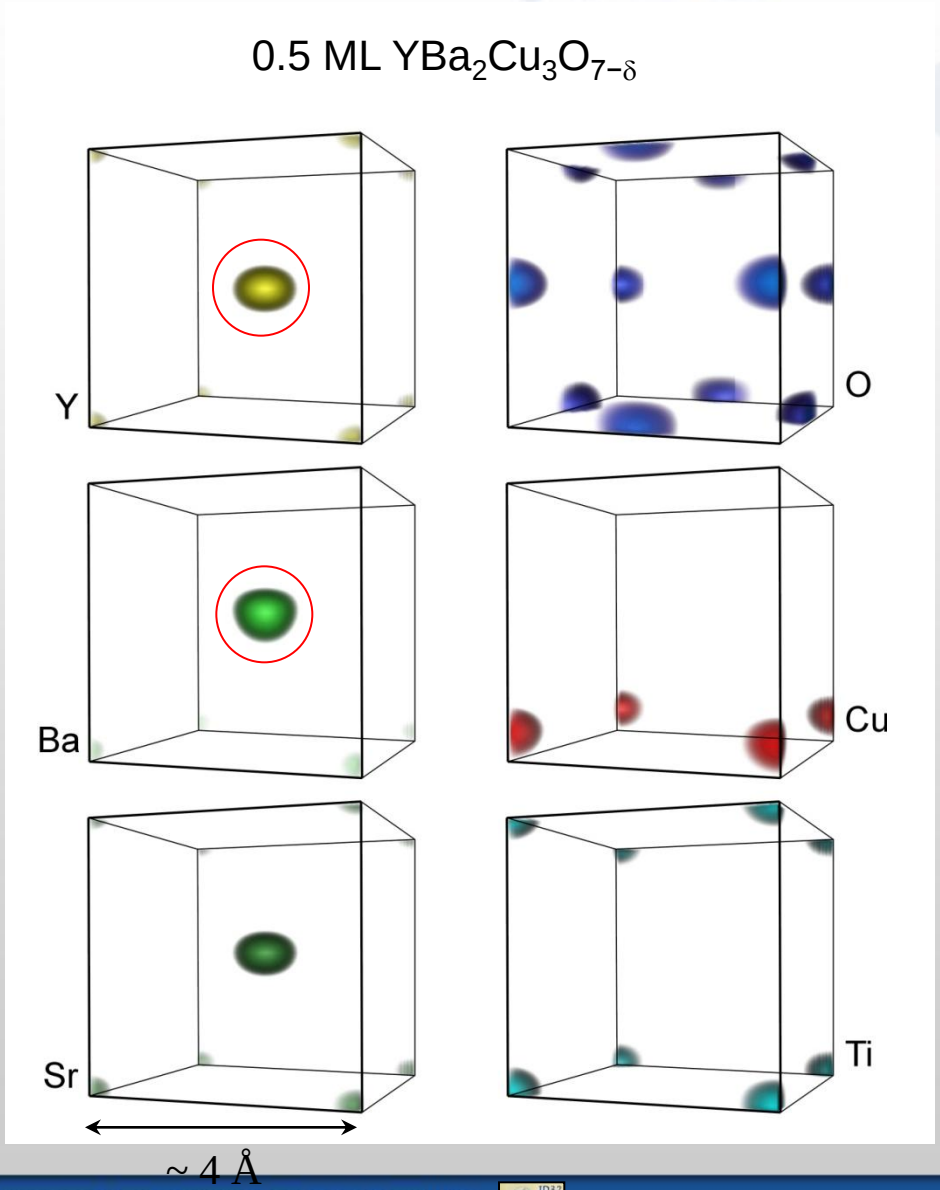

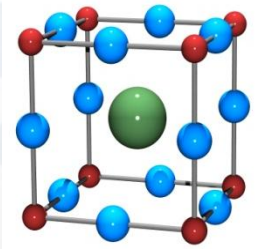

Perovskite structure

- perovskite structure
- oxygen visible
- 2 distinct layer spacings
- Y and Ba occupy different sites

projections into the $SrTiO_3$ unit cell

LAO/STO interface

Conductive interfaces between the insulating oxides $LaAlO_3$ (LAO) and $SrTiO_3$ (STO)

- Sharp interface
- Critical thickness >4uc

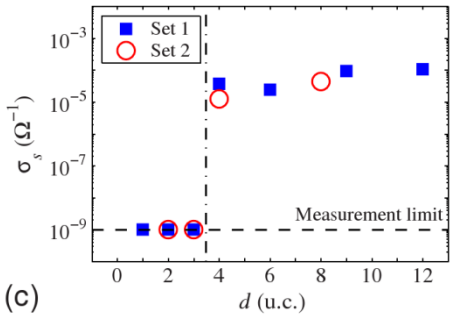

Electronic properties

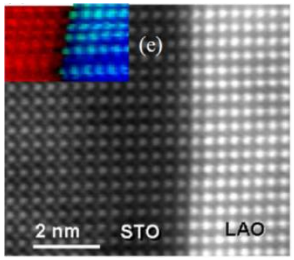

STEM

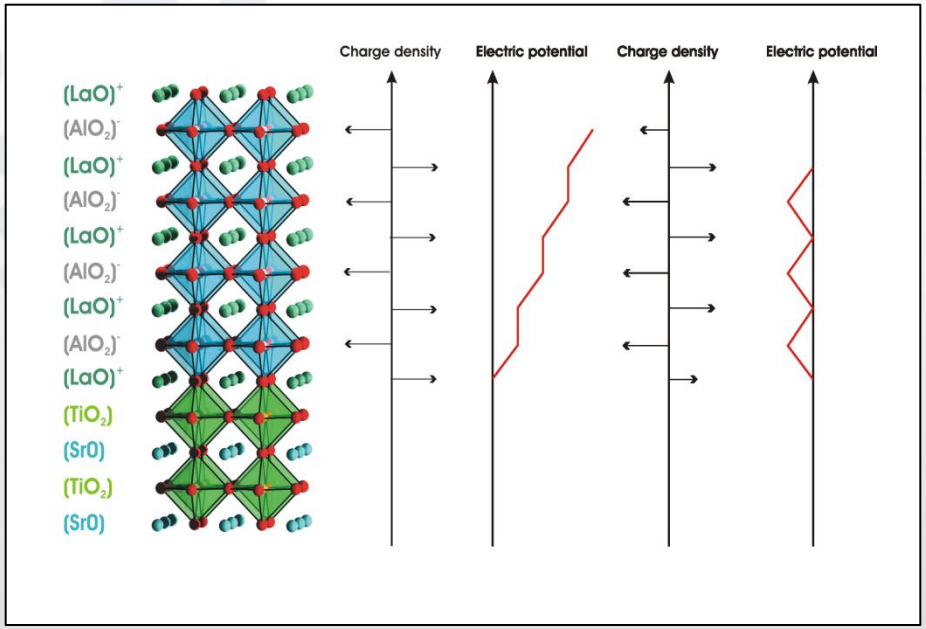

Growth conditions:

$pO_2 = 10^{-3}$ mbar

T = 800°C

F = 2 J/cm^2

Sheet carrier density:

~ 3 x 10^{14} cm^{-2}

Possible reasons :

Cation intermixing

O-vacancies

Valence change / intrinsic e^- doping

Lattice distortions

C. Aruta et al., Appl. Phys. Lett. 97, 252105 (2010)
R. Perna et al., Appl. Phys. Lett. 97, 152111 (2010)
A. Savoia et al., Phys. Rev. B 80, 075110 (2009)

→ Lattice distortion : This can be measured with XSW

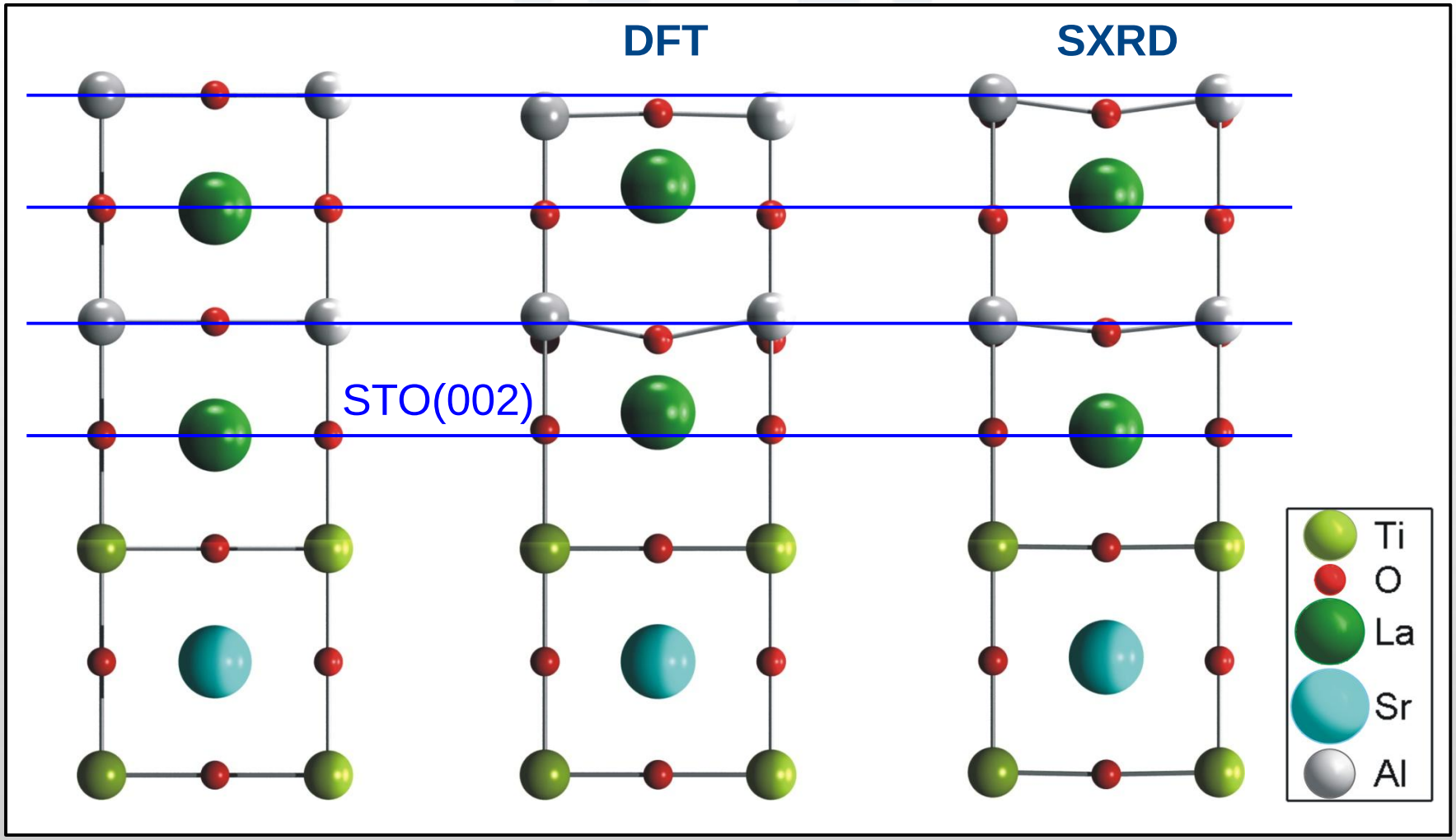

Qualitative images similar to:
DFT: R. Pentcheva and W.E. Pickett, PRL 102, 107602 (2009)
SXRD: S. A. Pauli et al., PRL 106, 036101 (2011)

Imaging of a 2uc LAO film

(h k l)	Al1s		La3d		O1s		Ti2p		Sr3s	
	fH	PH	fH	PH	fH	PH	fH	PH	fH	PH
1 1 1	0.92	0.57	0.68	0.95	0.66	0.94	0.90	0.53	0.90	0.99
1 1 2	0.21	0.88	0.66	0.02	0.25	0.53	0.99	1.00	0.96	0.99
0 0 2	0.42	0.93	0.73	0.03	0.64	1.00	1.08	0.01	0.82	0.99
2 0 2	0.54	0.96	0.61	0.01	0.45	0.02	0.94	0.99	1.01	0.00
1 0 3	0.36	0.93	0.70	0.05	0.41	0.47	1.02	0.02	0.92	0.01
1 1 3	0.50	0.43	0.63	0.01	0.88	0.02	1.10	0.50	0.82	0.02
1 2 1	0.34	0.83	0.56	0.94	0.39	0.62	1.05	0.99	--	--

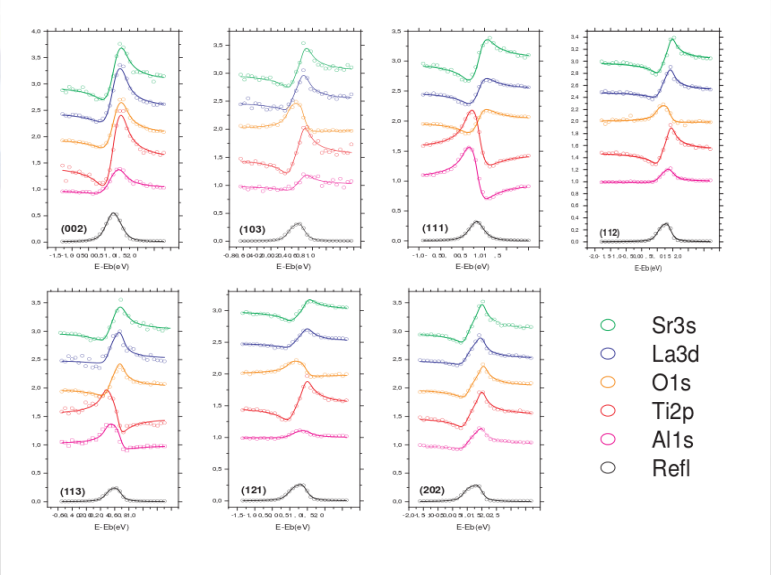

The film will follw the substrate symmetry. Im3m → P4mm

We can apply the 4-fold symmetry of the surface to our results and obtain **27 Fourier components** of the atomic distribution function for *each* element.

Multipicity:

(111),(112),(113), (103),(202)	4
(002)	1
(211)	8

Imaging of a 2uc LAO film

Direct Fourier Transform

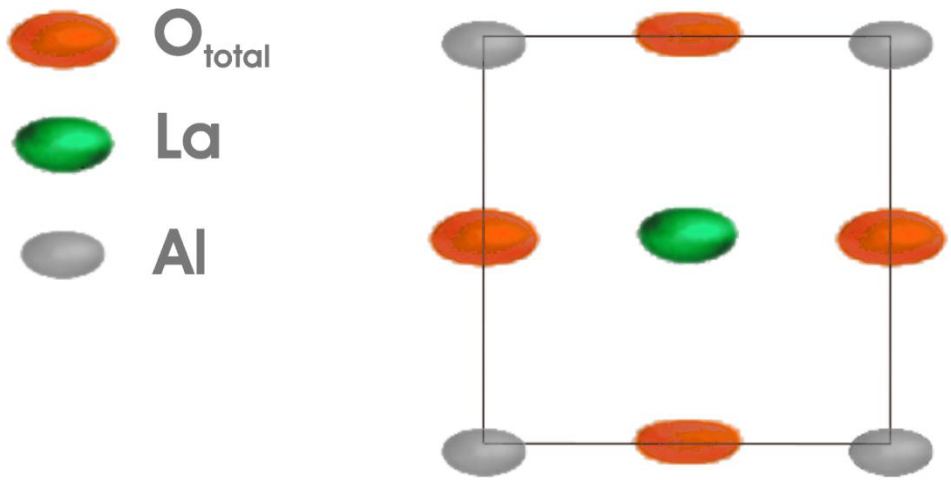

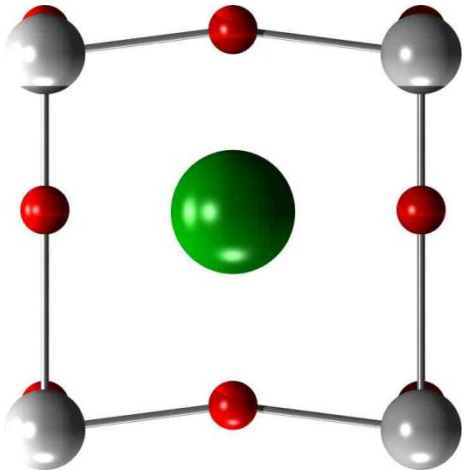

Measured displacement x2

Reconstruction of "image" via :

$$\rho(\mathbf{r}) = 1 + 2\sum_{\mathbf{H}} f^{\mathbf{H}} \cdot \cos\left[2\pi\left(P^{\mathbf{H}} - \mathbf{H}\cdot\mathbf{r}\right)\right]$$

Displacements :

Al	**- 10 pm**
La	**+ 5 pm**
O_{total}	**+ 2 pm**

Contains contribution from bulk STO oxygen

Site specific photoelectron emission

Site-specific decomposition of the $SrTiO_3$ valence band

Valence Yield excited by

1) ... a single X-ray beam:

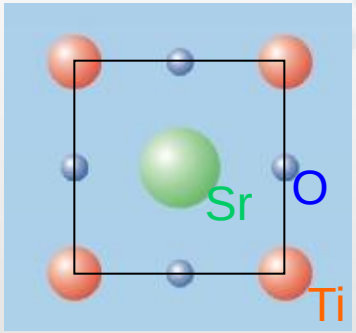

$SrTiO_3$

$$Y_{VB}(E_B) = \left\{ \sum_{j = Sr, Ti, O_3} Y_j(E_B) \right\}$$

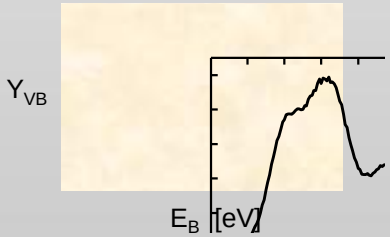

2) ... an XSW field:

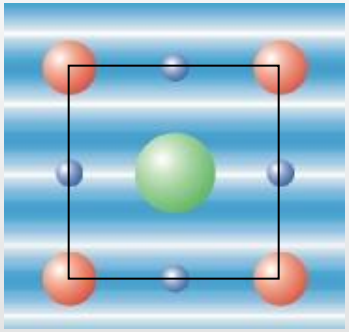

$$Y_{VB}(E_B, E_\gamma) = \sum_{j = Sr, Ti, O_3} I_j(E_\gamma)\, Y_j(E_B).$$

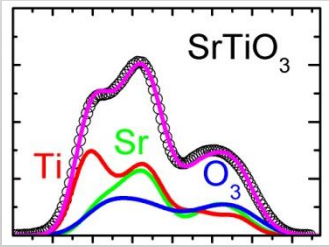

Oxygen Vacancies

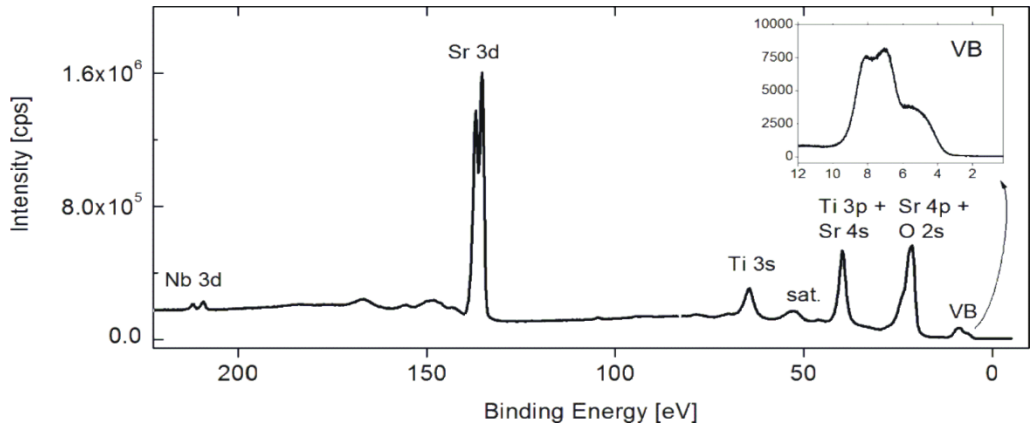

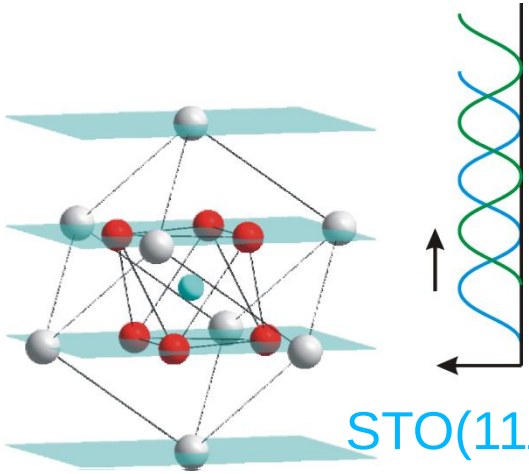

STO(111)
@2.75keV

→ Oxygen vacancies play a role in the conduction mechanism

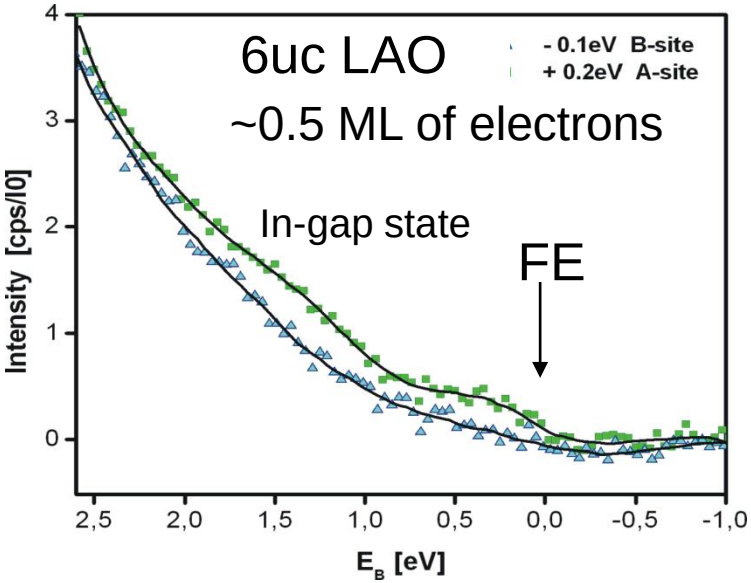

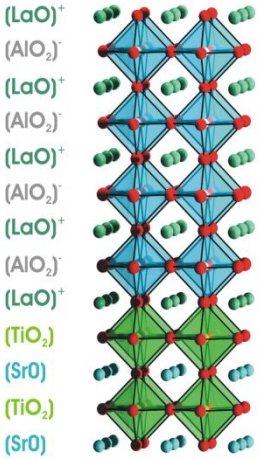

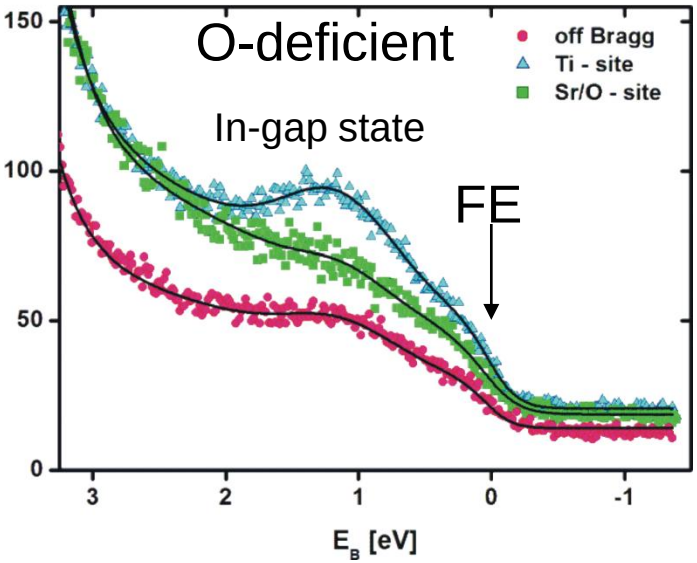

Beyond element specificity

- Probing chemical states through core-level binding energy shifts

Electron Spectroscopy for chemical analysis ESCA

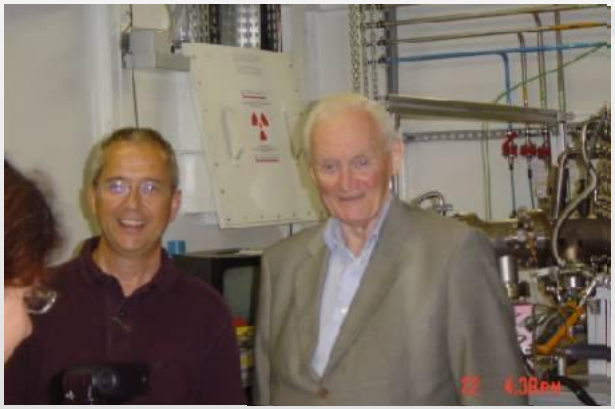

Nobel Prize 1981

† 20 July 2007 (aged 89)

Kai M. Siegbahn
at the ESRF at
ID32 in 2004

Ethyl trifluoroacetate

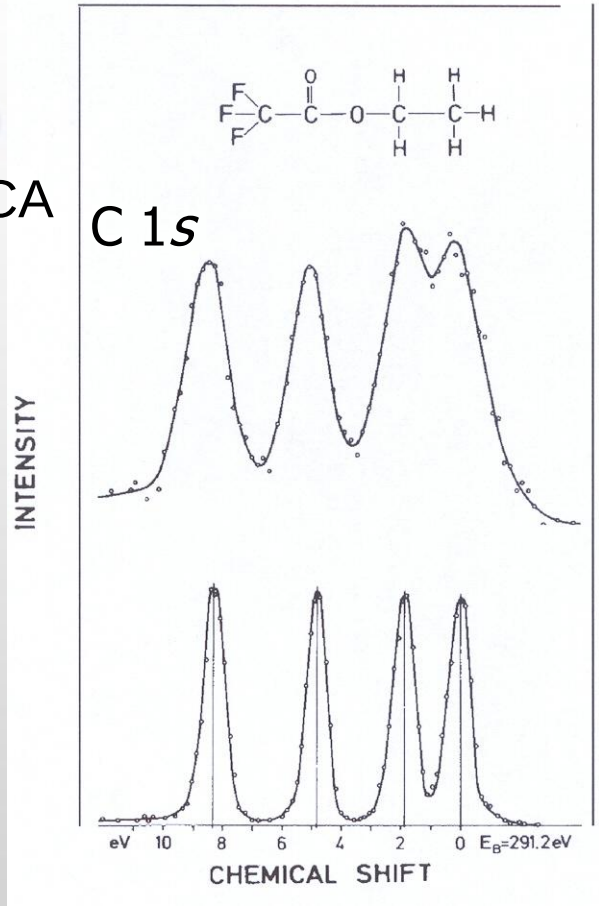

U. Gelius, E. Basilier, S. Svensson, T. Bergmark and K. Siegbahn, J. Electron Spectrosc. ***2****, 405 (1974)*

Combine core-level shift detection with XSW:

M. Sugiyama, S. Maeyama, S. Heun, and M. Oshima, PRB ***51****, 14778 (1995) – Sulfur passivated GaAs(001)*

G.J. Jackson, D.P. Woodruff, R.G. Jones, N.K. Singh, A.S.Y. Chan, B.C.C. Cowie, and V. Formoso, PRL ***84****, 119 (2000) – CH_3SH/Cu(111)*

Molecular Distortions and Chemical Bonding of PTCDA/Ag(111)

*A. Hauschild, K. Karki, B. C. C. Cowie, M. Rohlfing, F. S. Tautz, and M. Sokolowski, PRL **94**, 036106 (2005)*

3,4,9,10-perylene-tetracarboxylic-dianhydride

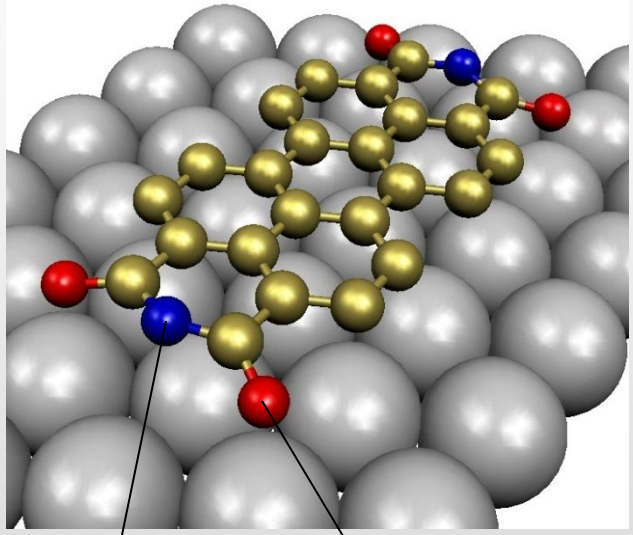

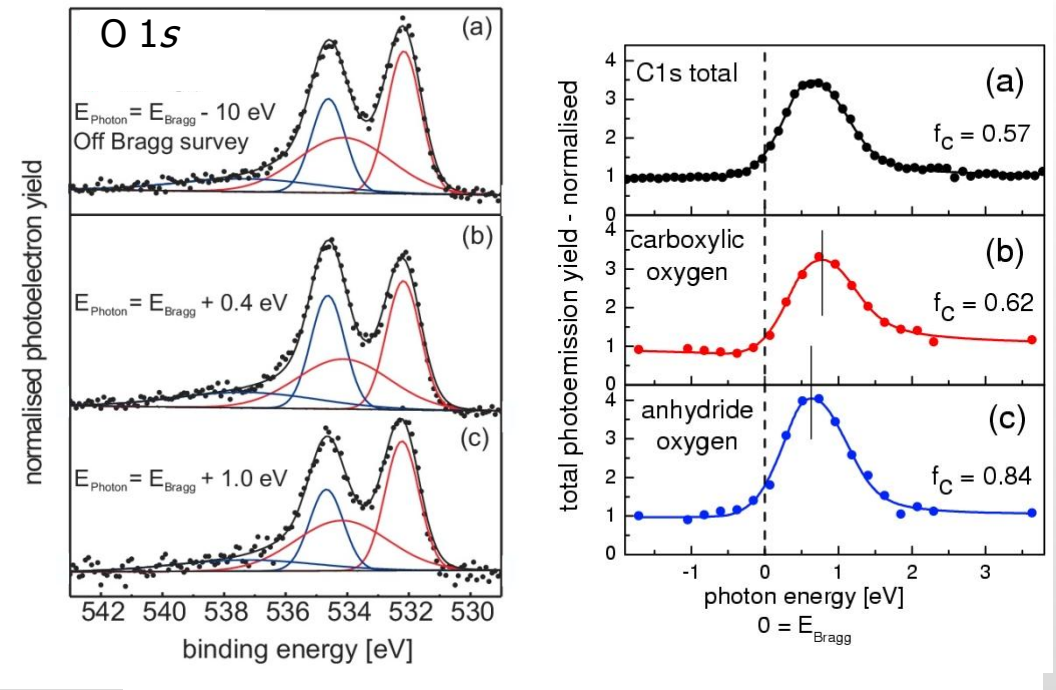

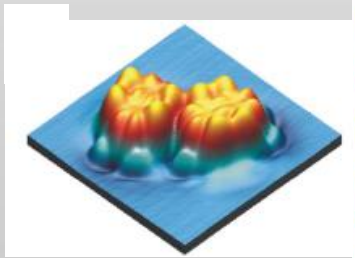

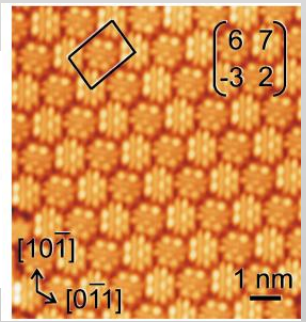

Hauschild et al., ESRF Highlights 2005

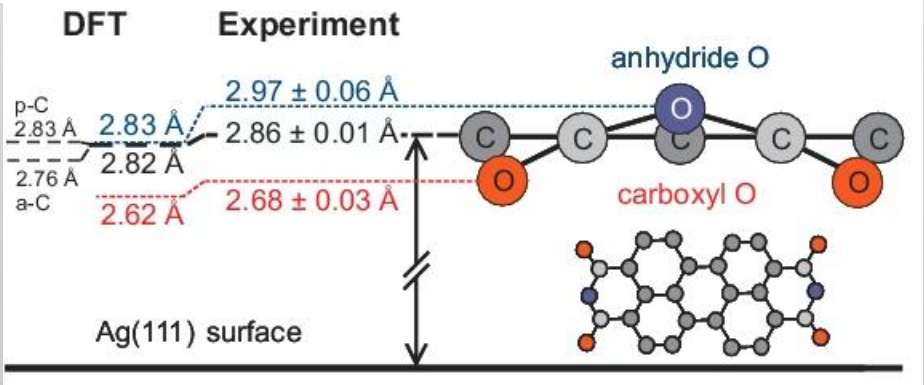

The α-Sn/Ge(111) surface

VOLUME 79, NUMBER 15 PHYSICAL REVIEW LETTERS 13 OCTOBER 1997

Surface Charge Ordering Transition: α Phase of Sn/Ge(111)

J. M. Carpinelli,[1] H. H. Weitering,[1] M. Bartkowiak,[1] R. Stumpf,[2] and E. W. Plummer[1]

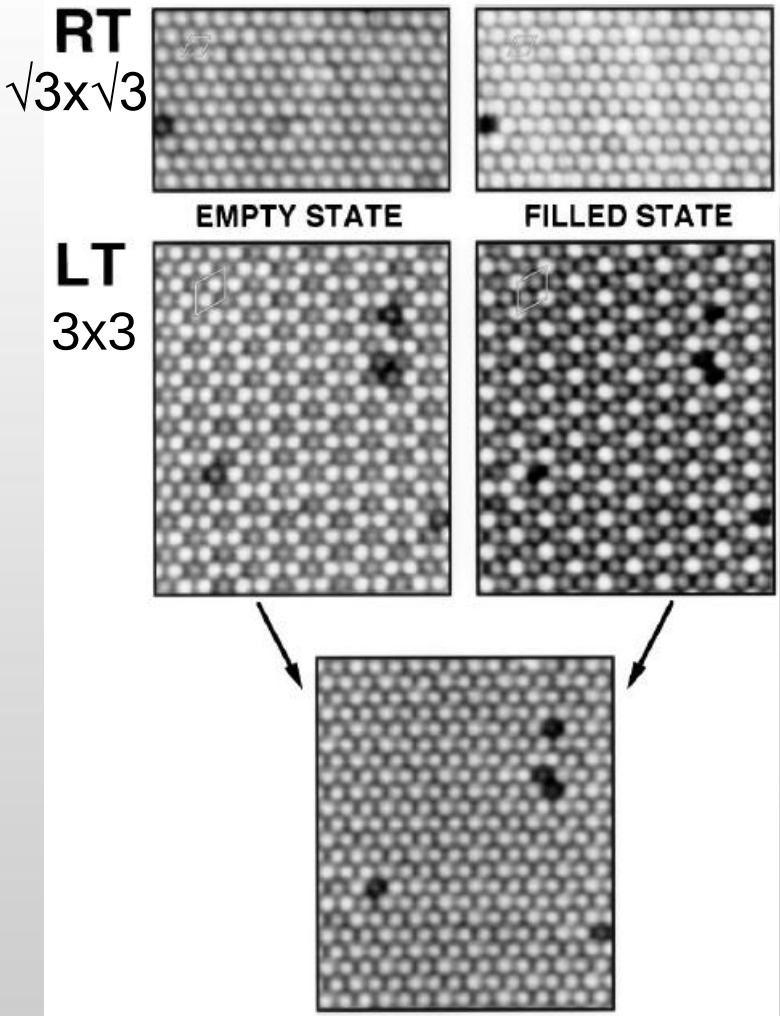

1. Registry aligned 105 × 60 Å² STM images sh

M. Goshtasbi Rad et al. / Surface Science 477 (2001) 227–234

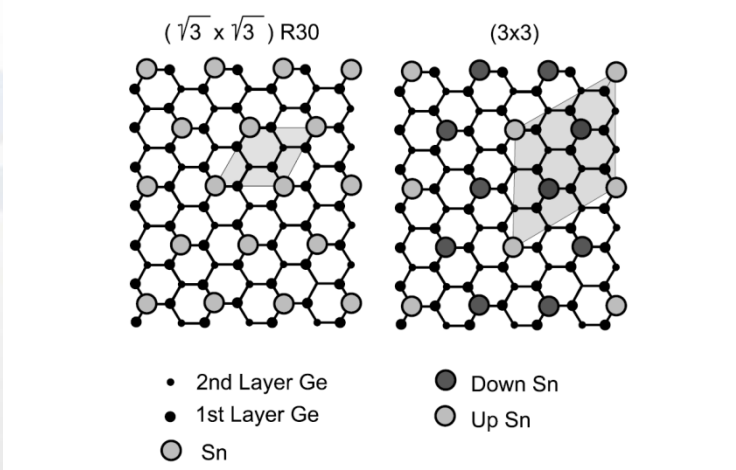

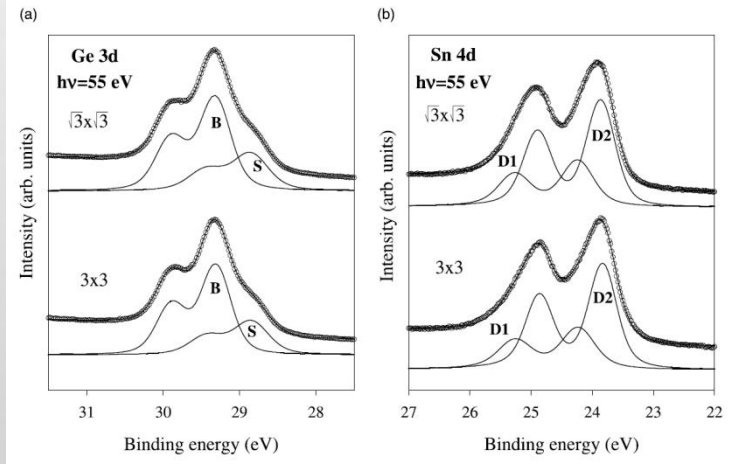

Combine core-level shift detection with XSW

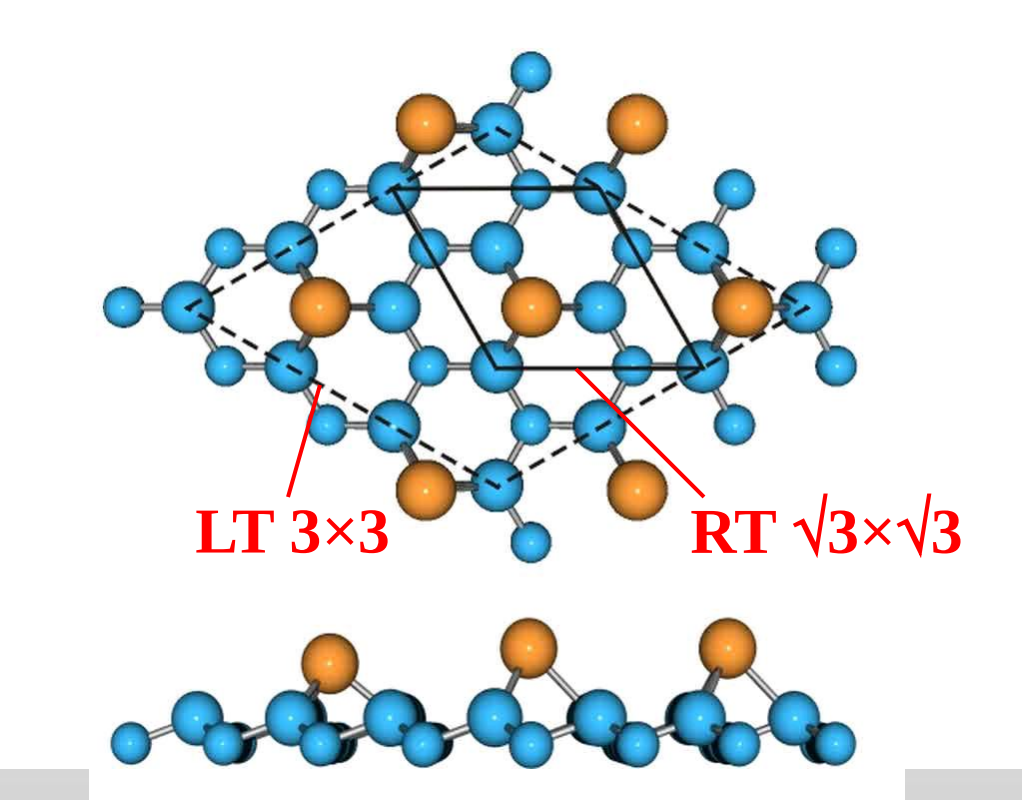

α-Sn/Ge(111) surface

- A seemingly simple structure: **T_4 site** adsorption of 1/3 ML of Sn adatoms
- **Electron counting of dangling bond per surface unit cell**
  ⇒ Metallic and unstable ??
- RT √3×√3 ↔ LT 3×3 phase transition at ~ 200 K
- Main question: **structure of the RT phase**

* *Fluctuation model: J. Avila et al., PRL **82**, 442 (1999).*

* *Calculations: G. Ballabio et al., PRL 89, 126803 (2002)*

RT Sn/Ge(111) probed by **hard x-ray photoelectron spectroscopy**

(hν = 2510 eV with ΔE ~ 500 meV)

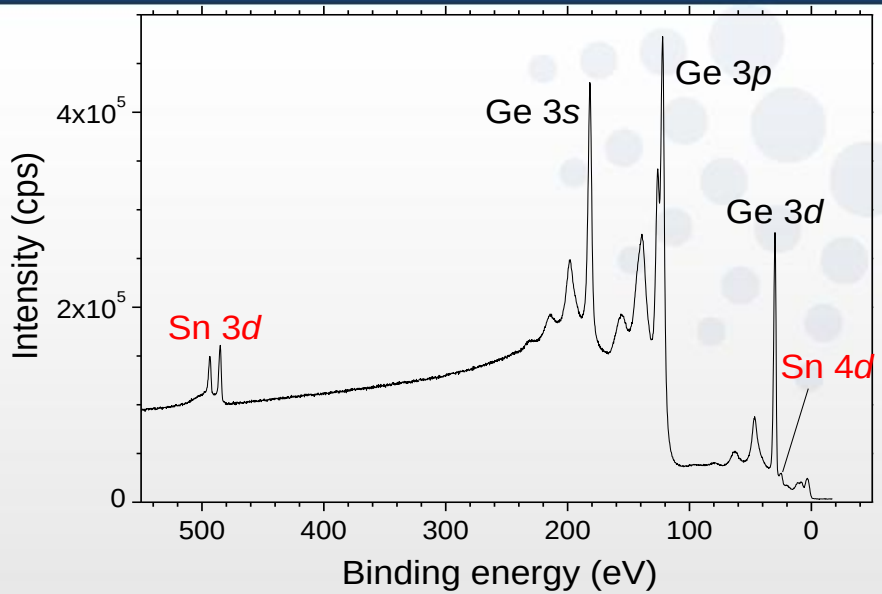

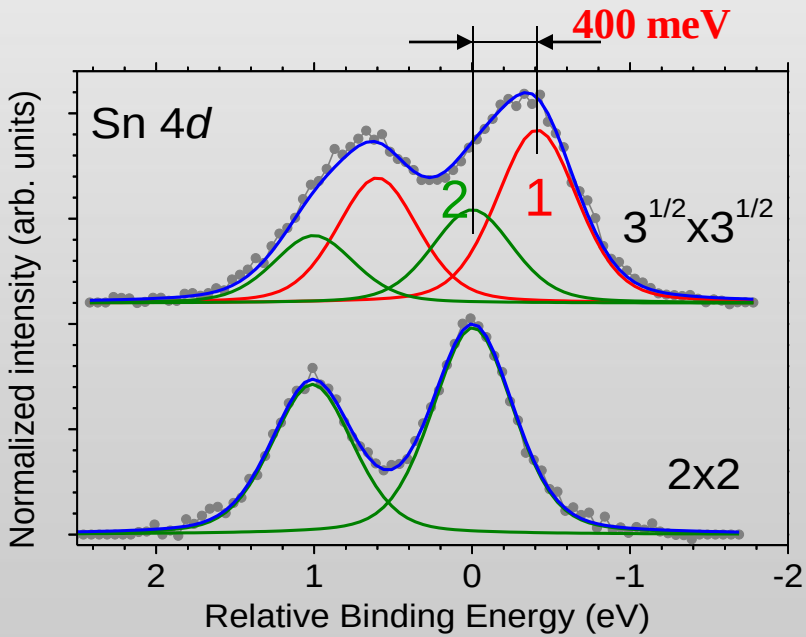

$\sqrt{3}\times\sqrt{3}$ (1/3 ML)

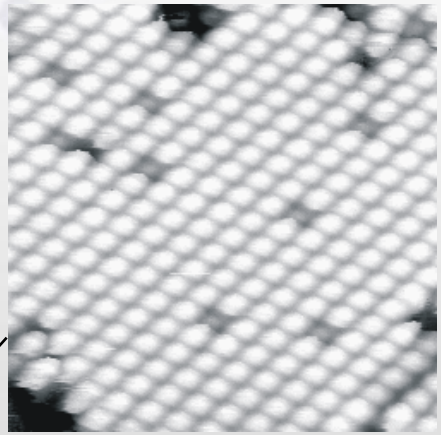

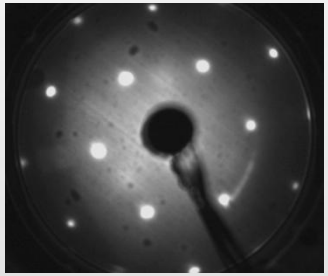

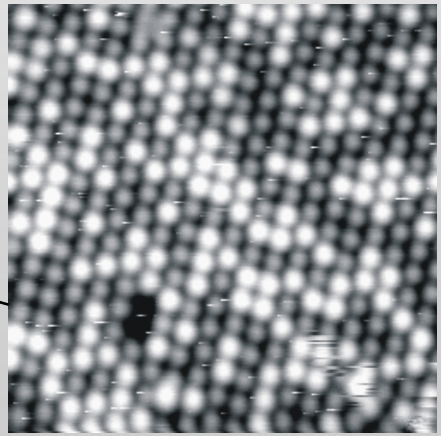

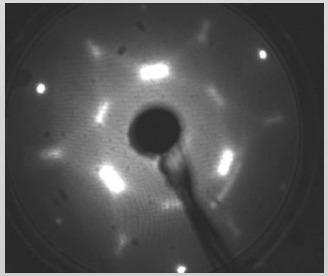

2x2 (< 0.2 ML)

RT Sn 4*d* core-level spectra modulated by Ge(111) XSW

(normalized to the peak height)

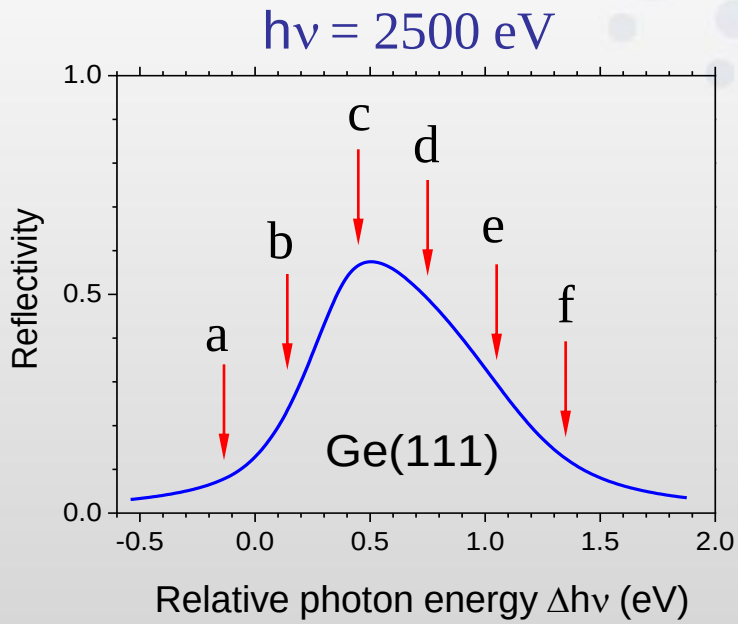

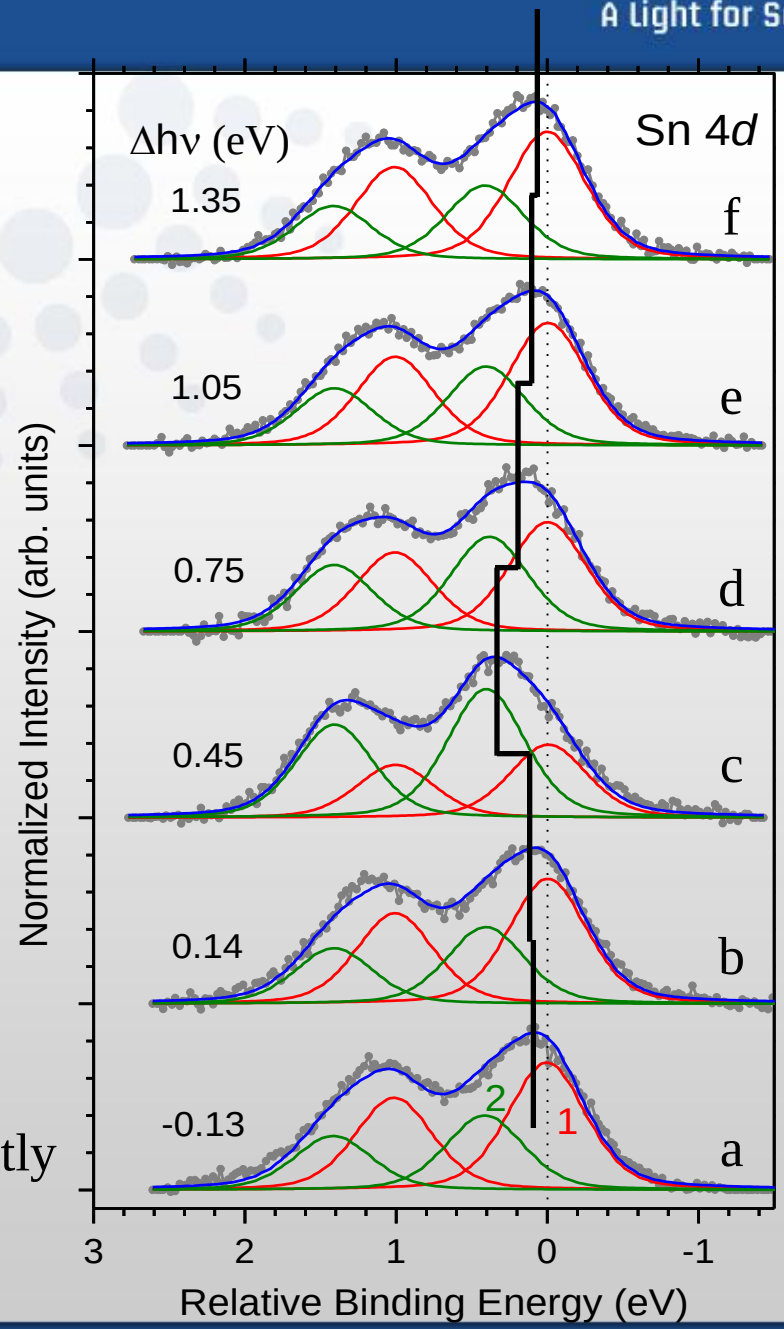

Intensity ratio I_1/I_2 varies with hν

⇒ Sn 1 & 2 are modulated differently

⇒ **2 Sn sites**

RT investigation of Sn 3*d* core-level shift

E = 2.5 keV ± ΔE

Core hole lifetime width of Sn 3d ~ 400 meV

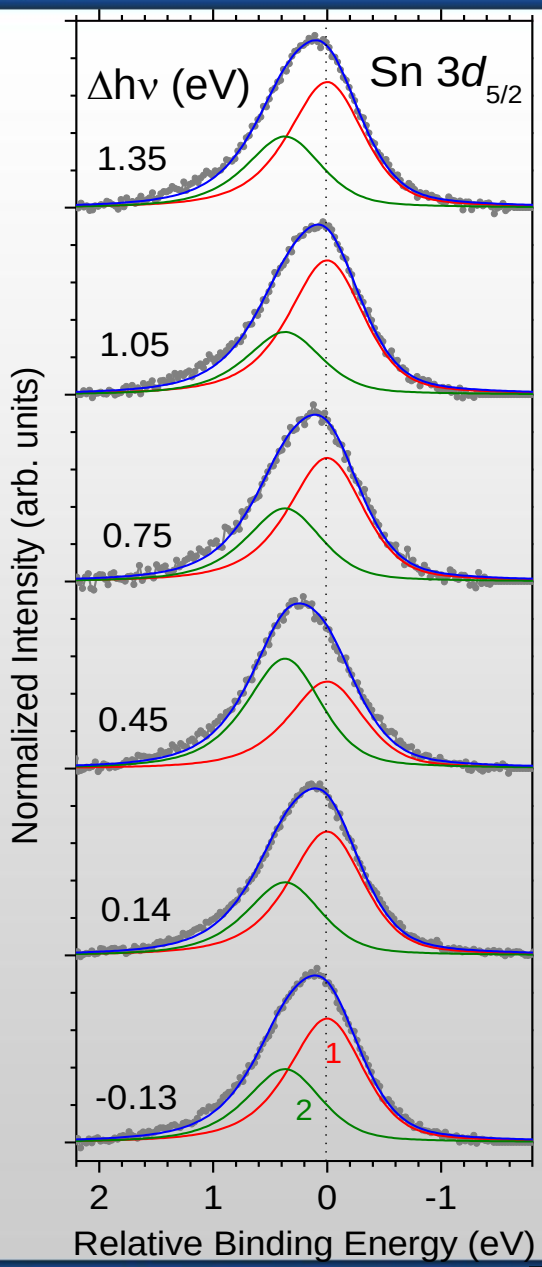

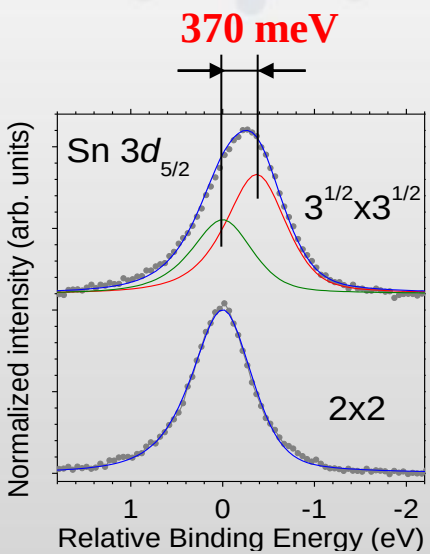

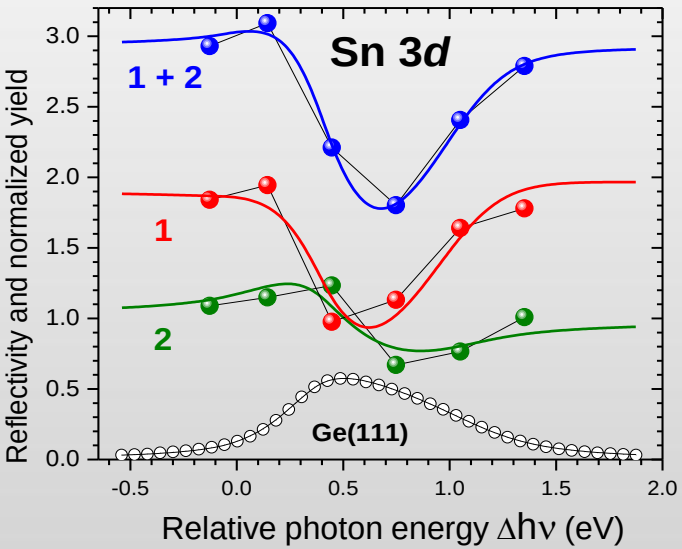

<= Ge(111) XSW modulated spectra

Ge(111):Sn RT √3x√3 – XSW/XPS Analysis

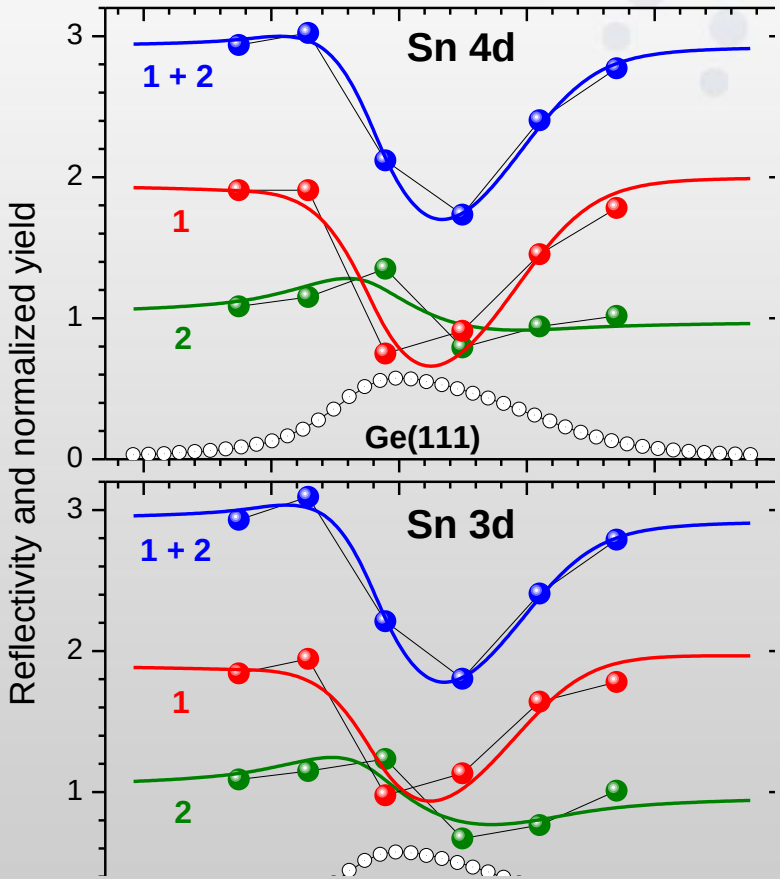

	Comp	f_{111}	P_{111}	I_1/I_2	h (Å)	Δh (Å)
3*d*	1+2	*0.66*	*0.78*	***1.92***	*2.55*	***0.23***
	1	*0.75*	*0.80*		*2.61*	
	2	*0.52*	*0.73*		*2.38*	
4*d*	1+2	*0.68*	*0.79*	***1.96***	*2.58*	***0.23***
	1	*0.86*	*0.80*		*2.61*	
	2	*0.40*	*0.73*		*2.38*	

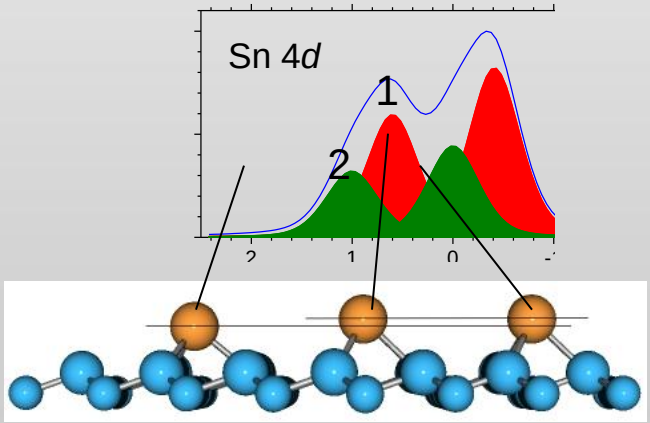

T.L. Lee, B.C.C. Cowie, S. Warren, J. Zegenhagen, Phys. Rev. Lett. **96,** 046103 (2006)

Ge(111):Sn RT √3x√3 – XSW/XPS Analysis

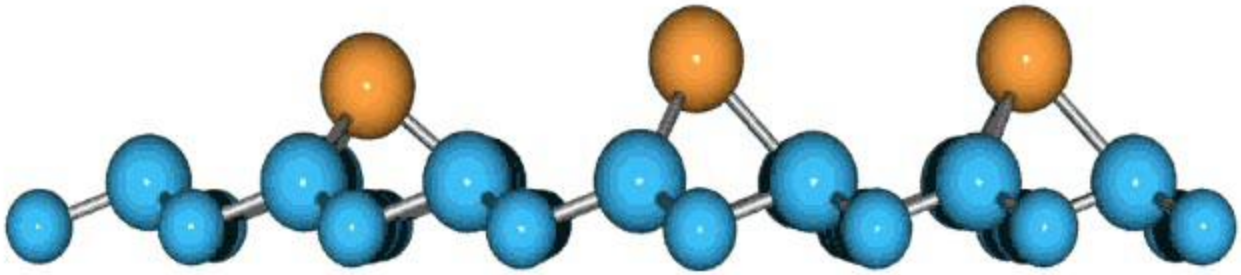

A seemingly simple structure: **T4 site** adsorption of 1/3 ML of Sn adatoms, but atoms occupy two different heights and flip fast and thus appear to be equivalent e.g. in STM images

Concluding Remarks

- XSW very powerful in combination with spectroscopy
- With proper instrumentation, XSW imaging is routine
- Further combinations of XSW with spectroscopy expected (ARPES, RIXS, …) also microscopy (presently 5 µm)
- HAXPES, a powerful technique in its own right, combines excellently with the XSW technique
- Importance of auxiliary support laboratories
- Consider efficient use of beamtime; allow staff to do the best science; however, think careful about multi-technique capability for a state-of-the-art beamline because of sophistication of set-ups

HAXPES/XSW workshop at the ESRF : February 6-8, 2012

Acknowledgement

Lina Aruta, *Univ. Tor-Vergata, Rome*
Carsten Busse, *University Cologne*
Francois Bottin, *CEA/DAM Ile-de-France*
Bruce C.C.Cowie, *Australian Light Source*
Tien-Lin Lee, *DIAMOND Light Source*
Olaf Magnussen, *Univ. Kiel*
Sebastian Thiess, *HASYLAB/DESY*
German BMBF (€€€)

ID32 staff

Lionel André	Technician
Blanka Detlefs	Scientist
Julien Duvernay	Post-Doc
Éric Gagliardini	Engineer
Hadeel Hussain	PhD
Helena Isern	Scientist
Manuel Perez	Engineer
Parasmani Rajput	Post-Doc
Jérôme Roy	Scientist
Christoph Schlueter	PhD

Thank you for your attention

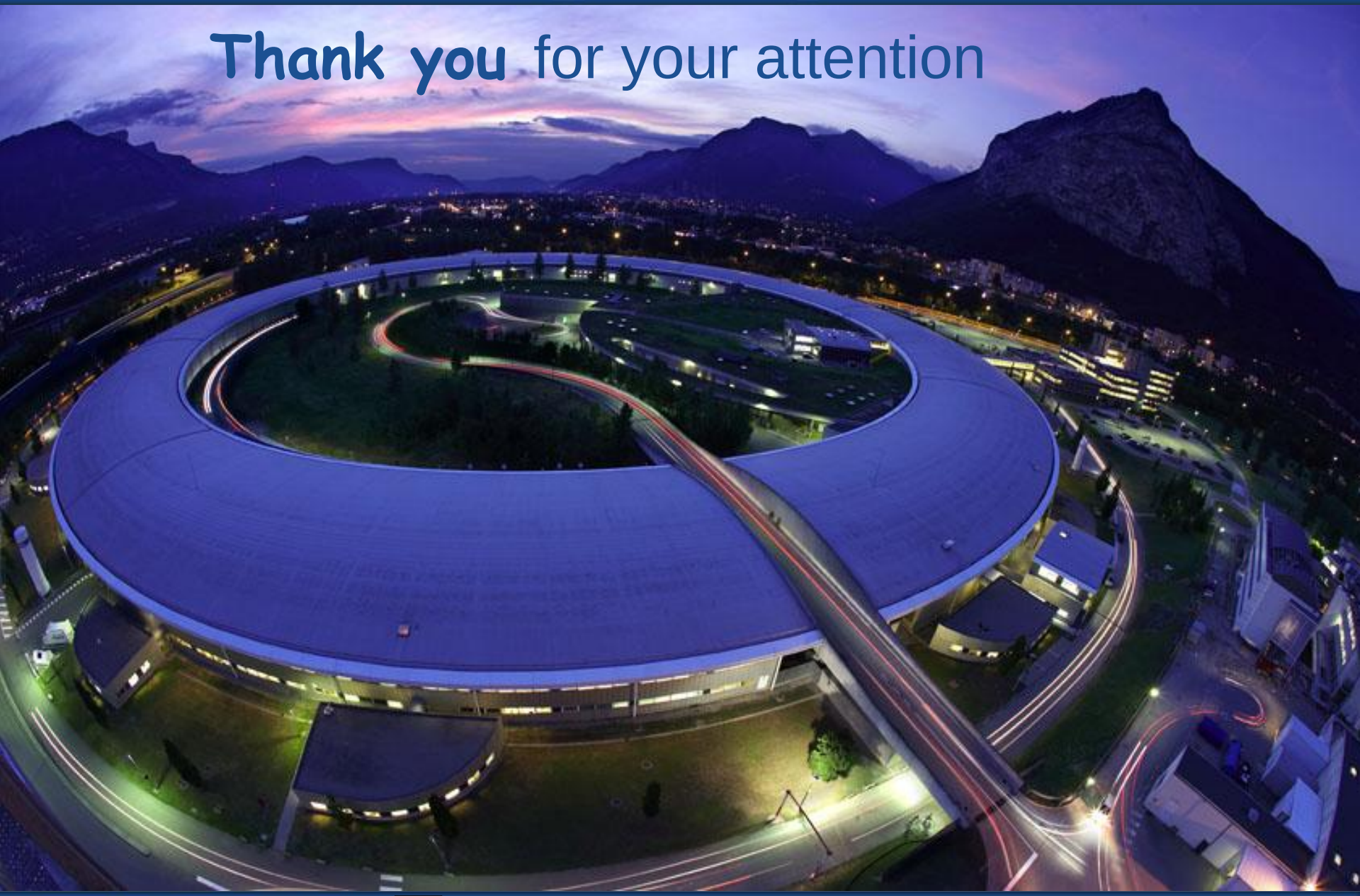

A Light for Science

European Synchrotron Radiation Facility